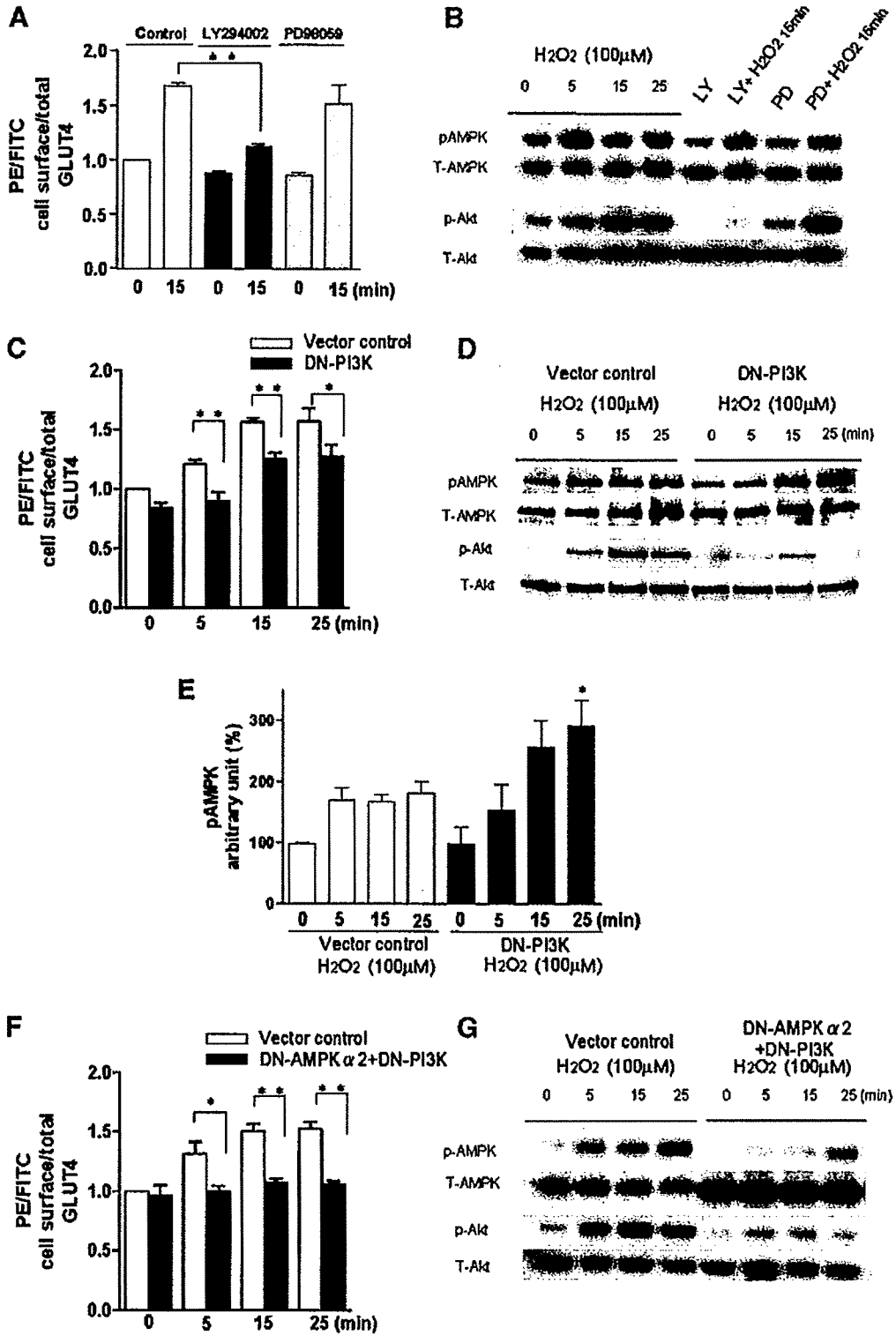

Fig. 4. Effects of PI3 kinase inhibition on H_2O_2-induced GLUT4 translocation. The translocation of GLUT4 in the plasma membrane was measured by flow cytometry as described in the Materials and Methods Section. The level of GLUT4 translocation without treatment was set at 1.0. Values are the means ± SE of four to eight independent experiments. A: H_2O_2-induced GLUT4 translocation was measured by FACS analysis. LY294002 (50 μM) inhibited H_2O_2-induced GLUT4 translocation as measured by FACS analysis at 15 min after exposure to H_2O_2 ($P < 0.01$). PD98059 (20 μM) did not inhibit GLUT4 translocation. B: Western blot analysis indicated that H_2O_2-induced Akt activation was inhibited by LY294002 but not by PD98059. C: Dominant-negative PI3-K (DN-PI3K) inhibited H_2O_2-induced GLUT4 translocation as measured by FACS analysis (*$P < 0.05$, **$P < 0.01$). D: Western blot analysis indicated that H_2O_2-induced Akt activation was inhibited by the expression of DN-PI3-K. E: Effect of DN-PI3-K expression on H_2O_2-induced AMPK phosphorylation (*$P < 0.05$). Densitometric analysis was performed on the level of AMPK phosphorylation. The mean basal level of AMPK phosphorylation of vector control was set at 100%. Values are the means ± SE of four independent experiments. F: The DN of AMPKα2 and DN-PI3-K inhibited GLUT4 translocation as measured by FACS analysis (*$P < 0.05$, **$P < 0.01$). G: Western blot analysis indicated that H_2O_2-induced AMPK and Akt activation were inhibited by the expression of DN of AMPKα2 and DN-PI3-K.**

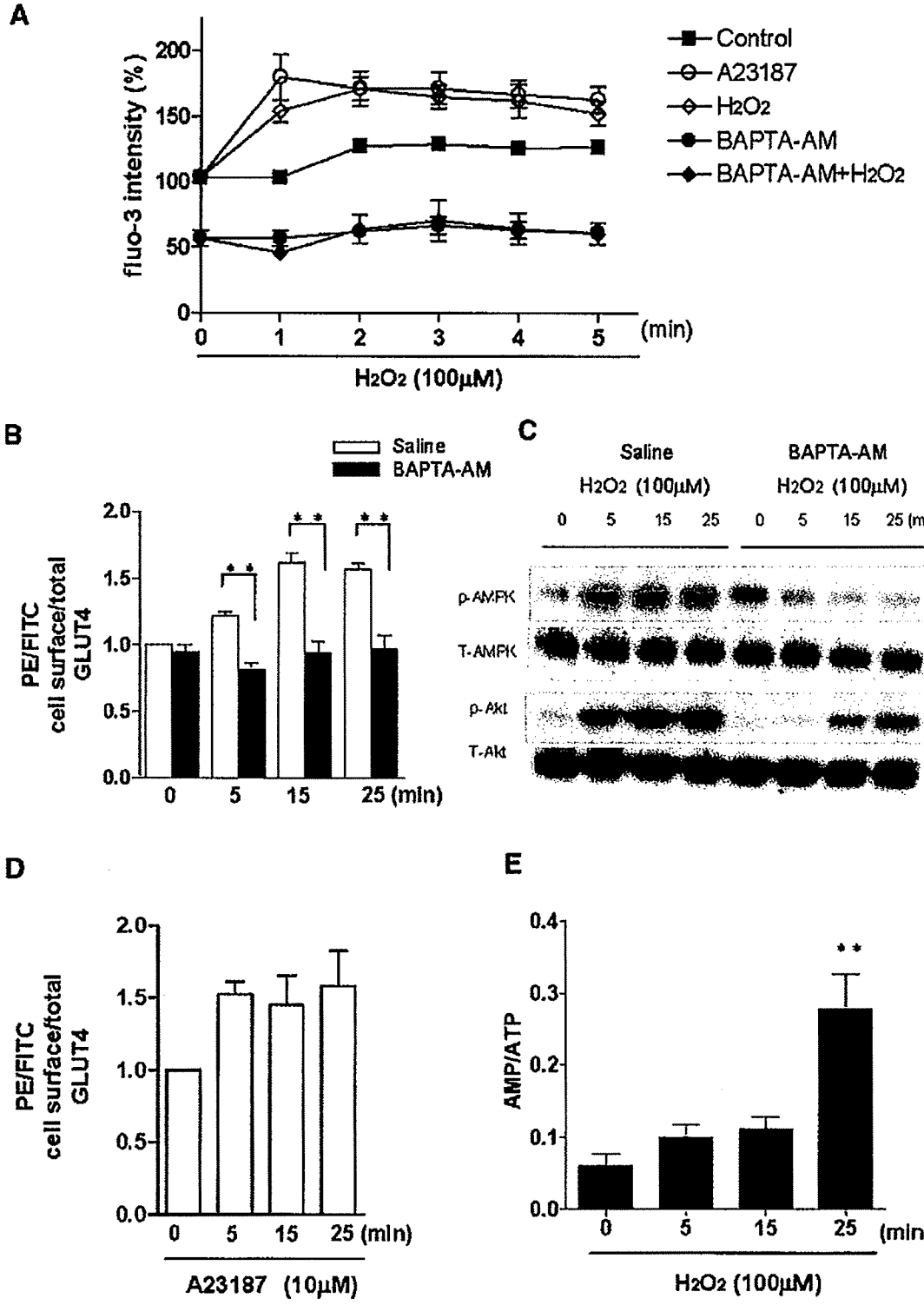

Fig. 5. H_2O_2-induced increase in the intracellular Ca^{2+} concentration ($[Ca^{2+}]i$) and AMP/ATP ratio. A: Relative changes in $[Ca^{2+}]i$ were measured by fluo-3-AM. H_2O_2 induced an increase in $[Ca^{2+}]i$ within 1 min. Pretreatment with BAPTA-AM (100 μM) completely inhibited this H_2O_2-induced increase in $[Ca^{2+}]i$. B: BAPTA-AM completely inhibited H_2O_2-induced GLUT4 translocation. C: Western blot analysis indicated that H_2O_2-induced AMPK and Akt activation were inhibited by pretreatment with BAPTA-AM. D: The calcium ionophore A23187 induced GLUT4 translocation to the same extent as H_2O_2. The level of GLUT4 translocation without treatment was set at 1.0. Values are the means ± SE of four to six independent experiments ($^*P < 0.05$, $^{**}P < 0.01$). E: Changes in the AMP/ATP ratio were measured by reversed-phase HPLC (Amersham Biosciences; $^{**}P < 0.01$).

these two DN-forms inhibited the H_2O_2-induced phosphorylation of AMPK. The effect of the simultaneous expression of these two DN-forms was almost comparable to that caused by the expression of DN-AMPKα2.

Effect of PI3K inhibition on H_2O_2-induced GLUT4 translocation

It is well known that PI3-K is necessary for insulin-induced GLUT4 translocation. Therefore, we also examined the effect of the PI3-K inhibitor LY294002 on GLUT4 translocation in cardiomyocytes. As shown in Figure 4A, LY294002 significantly inhibited GLUT4 translocation, whereas the ERK kinase inhibitor PD98059 had no effect. Figure 4B shows that H_2O_2 phosphorylates Akt, which was inhibited by treatment with LY294002. PD98059 had no effect on the H_2O_2-induced phosphorylation of Akt. Neither PD98059 nor LY294002 inhibited the H_2O_2-induced phosphorylation of AMPK. To further explore the role of PI3-K in H_2O_2-induced GLUT4 translocation, we expressed a mutant PI3-K (DN-PI3-K), which acts dominantly to inhibit the activation of PI3-K. We monitored H_2O_2-induced GLUT4 translocation at 0, 5, 15, and 25 min after stimulation and found that the expression of DN-PI3-K inhibited H_2O_2-induced GLUT4 translocation at every time-point examined (Fig. 4C). Expression of DN-PI3-K almost completely inhibited Akt phosphorylation. However, it did not inhibit the H_2O_2-induced phosphorylation of AMPK (Fig. 4D). Since previous studies have shown that Akt activation inhibits AMPK (Horman et al., 2006; Soltys et al., 2006), we further examined the interaction between these two kinases. When we measured the change in AMPK phosphorylation levels in response to H_2O_2 treatment, expression of DN-PI3-K significantly increased the level at 25 min after H_2O_2 stimulation (Fig. 4E). These findings suggest that H_2O_2-induced activation of PI3-K/Akt is required for the inhibition of AMPK phosphorylation, while H_2O_2 activates both AMPK and PI3-K/Akt at the same time. Finally, we tested the hypothesis that both AMPK and PI3-K/Akt are activated by H_2O_2 and contribute to GLUT4 translocation at the same time. When the DN of AMPKα2 was applied with DN-PI3-K, there was a complete reduction in the GLUT4 membrane level similar to that seen at the 0 time-point (Fig. 4F). The effect of DN of AMPKα2 and DN-PI3-K was confirmed by the inhibition of AMPK and Akt phosphorylation (Fig. 4G). These results demonstrate that AMPK and PI3-K/Akt have an additive effect on oxidative stress-mediated GLUT4 translocation.

The increase in the AMP: ATP ratio is a later event than the increase in the intracellular Ca^{2+} concentration after stimulation with H_2O_2

CaMKKα and CaMKKβ can each activate AMPK in a manner that is stimulated by Ca^{2+} and calmodulin (Hurley et al., 2005). Moreover, PI3-K/Akt is activated by intracellular Ca^{2+} fluxes in endothelial cells (Thomas et al., 2002). Since an increase in the intracellular Ca^{2+} concentration ($[Ca^{2+}]i$) has been reported as an early event after exposure to oxidative stress (Goldhaber and Weiss, 1992), we measured the change in $[Ca^{2+}]i$ in neonatal cardiomyocytes in response to H_2O_2 treatment. As shown in Figure 5A, H_2O_2 induced a rapid increase in $[Ca^{2+}]i$ that was blocked by pretreatment with BAPTA-AM. BAPTA-AM significantly reduced the translocation of GLUT4 almost completely to a level similar to that seen at the 0 time-point (Fig. 5B). This reduction of GLUT4 translocation was accompanied by the inhibition of AMPK and Akt phosphorylation (Fig. 5C). In contrast, A23187 induced GLUT4 translocation as early as 5 min after treatment (Fig. 5D). Since AMP activates AMPK via a direct allosteric mechanism and by inhibiting the dephosphorylation of AMPK (Sanders et al., 2007), we also measured ATP, ADP, and AMP in cardiomyocytes by an HPLC-based method. Figure 5E shows that the change in the AMP: ATP ratio is not evident until 15 min after treatment with H_2O_2. However, these ratios increased dramatically at 25 min after stimulation.

Peroxynitrite induces a rapid translocation of GLUT4

We also examined the effect of oxidative stress by $ONOO^-$ on GLUT4 translocation. $ONOO^-$ induced GLUT4 translocation in neonatal cardiac myocytes (Fig. 6A). Treatment with $ONOO^-$ activated both AMPK and Akt in the same way as with H_2O_2 (Fig. 6B).

Discussion

The goal of the present study was to further elucidate the precise mechanism that links oxidative stress and GLUT4 translocation in cardiomyocytes.

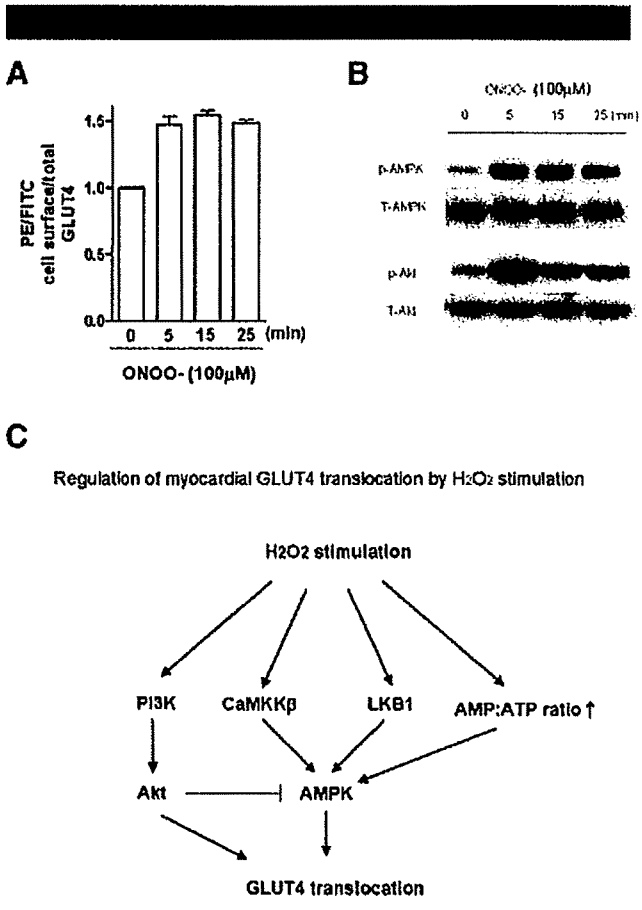

Fig. 6. Oxidative stress and GLUT4 translocation. A: Oxidative stress by $ONOO^-$ induced GLUT4 translocation in neonatal cardiac myocytes. The translocation of GLUT4 in the plasma membrane was measured by flow cytometry as described in the Materials and Methods Section. The level of GLUT4 translocation without treatment was set at 1.0. Values are the means ± SE of four to eight independent experiments. B: Western blot analysis indicated that oxidative stress by $ONOO^-$ induced AMPK and Akt activation. C: Proposed link between H_2O_2 and GLUT4 translocation in cardiomyocytes. Exposure to H_2O_2 (similar to an increase in ROS during ischemia reperfusion) results in a rapid activation of AMPK and PI3-K/Akt in an earlier phase. A subsequent increase in the AMP: ATP ratio activates AMPK in a later phase.

Lentiviral-mediated transduction of GLUT4 reporter gene

Several assays for GLUT4 trafficking at the cell surface have been described. The subcellular fractionation protocol for measuring cell-surface GLUT4 is laborious, and the accurate quantitation has been difficult because of the cross-contamination of plasma membrane fractions (Cushman and Wardzala, 1980; Suzuki and Kono, 1980). The use of photoactivatable bismannose compounds to selectively tag cell-surface glucose transporters is also laborious and requires quantitative immunoprecipitation and analysis by SDS–PAGE (Yang et al., 1992; Satoh et al., 1993). Expression of an exogenous, tagged GLUT4 reporter offers greater flexibility in detection and quantitation (Bogan et al., 2001). In this method, the level of expression of such reporter protein is critical. Therefore, we used a lentiviral vector for efficient transduction of the GLUT4 reporter gene to neonatal rat cardiomyocytes. Previous reports have suggested that lentivirus vectors efficiently transduced and expressed genes for extended periods of time in cardiomyocytes both in vitro and in vivo (Zhao et al., 2002). Vectors based on lentiviruses have many advantages for gene therapy, including the ability to infect nondividing cells, long-term transgene expression and the absence of induction of an inflammatory/immune response (Sakoda et al., 1999). We could transduce GFP to more than 90% of cardiomyocytes and this is a simple, relatively rapid and quantitative method for monitoring GLUT4 translocation in cardiomyocytes.

Activation of two kinases upstream of AMPK

To test whether AMPK is involved in H_2O_2-induced GLUT4 translocation, a dominant-negative mutant of AMPKα2 (DN-AMPKα2) was expressed in cardiomyocytes by lentivirus. The dominant-negative form of AMPKα2, which abolishes AMPK activity, also inhibited the H_2O_2-induced translocation of GLUT4. LKB1 was recently identified as a major upstream kinase in the AMPK cascade (Hawley et al., 2003; Woods et al., 2003). AMPK is also activated by CaMKK (Woods et al., 2005). Therefore, we further tried to determine the involvement of these two upstream kinases in H_2O_2-mediated GLUT4 translocation in cardiomyocytes. A previous report suggested that the Ca^{2+}-mediated pathway of AMPK activation is most likely to play an important role in neuronal tissue since the expression of CaMKKα and CaMKKβ is much higher in the brain than in other organs (Hawley et al., 2005). Although CaMKK isoforms were determined to be expressed in heart, it is still unknown whether CaMKKs can activate AMPK (Anderson et al., 1998). In our experiment, we demonstrated that CaMKKβ is involved in GLUT4 translocation in cardiomyocytes, based on the finding that the CaMKKinhibitor STO-609, as well as overexpression of the dominant-negative form of CaMKKβ, inhibited its H_2O_2-mediated translocation.

Recent studies have suggested that a deficiency of LKB1 in the heart prevents ischemia-mediated activation of AMPKα2 but not AMPKα1 (Sakamoto et al., 2006). These findings indicate that LKB1 plays a crucial role in regulating the cellular energy level in response to ischemia. However, in our experiment, the expression of either DN-CaMKKβ or LKB1 did not have as great an effect as that induced by the simultaneous expression of both DN-CaMKKβ and LKB1 on H_2O_2-induced GLUT4 translocation. Therefore, both of these kinases are important for controlling GLUT4 translocation in cardiomyocytes.

Activation of PI3K/Akt pathway by H_2O_2

Since PI3-K/Akt-mediated signal transduction is known to be important for GLUT4 translocation and the PI3-K/Akt pathway is activated by H_2O_2 (Hill et al., 1999), we also tried to determine whether the PI3-K/Akt pathway is involved in H_2O_2-mediated GLUT4 translocation. The dominant-negative form of PI3-K or the PI3-K inhibitor LY 294002 significantly inhibited the H_2O_2-induced translocation of GLUT4 as well as the phosphorylation of Akt. Therefore, PI3-K/Akt-mediated GLUT4 translocation is also clearly demonstrated in our assay system.

AMPK and PI3K/Akt have an additive effect on H_2O_2-induced GLUT4 translocation

When the DN of AMPKα2 was applied with DN-PI3-K, there was a complete reduction in the GLUT4 membrane level similar to that seen at the 0-time point. These results are compatible with the data obtained in the experiment using BAPTA-AM to chelate intracellular calcium. Treatment with BAPTA-AM completely inhibited GLUT4 translocation as long as the inhibition of AMPK and Akt phosphorylation. The present study demonstrated that H_2O_2 activated both AMPK and Akt at the same time and AMPK and PI3-K/Akt have an additive effect on H_2O_2-induced GLUT4 translocation.

Several studies have shown that Akt activation inhibits AMPK (Horman et al., 2006; Soltys et al., 2006). When we measured the change in AMPK phosphorylation levels in response to H_2O_2 treatment, the expression of DN-PI3-K significantly increased the level at 25 min after H_2O_2 stimulation. Therefore, our results suggest that H_2O_2-induced PI3-K/Akt negatively regulates AMPK phosphorylation, while H_2O_2 activates both AMPK and PI3-K/Akt at the same time.

Proposed link between H_2O_2 and GLUT4 translocation in cardiomyocytes

Based on our results, we propose that oxidative stress causes the translocation of myocardial GLUT4 to the sarcolemma through AMPK activation by CaMKK and LKB1 together with PI3-K/Akt activation, which is followed by an increase in the AMP: ATP ratio. Exposure to H_2O_2 results in the rapid activation of AMPK and PI3-K/Akt, while Akt still inhibits AMPK activation in this situation (Fig. 6C).

CaMKKα and CaMKKβ can each activate AMPK in a manner that is stimulated by Ca^{2+} and calmodulin (Hurley et al., 2005). A rise in $[Ca^{2+}]i$ is required for Akt activation in endothelial cells (Thomas et al., 2002). In our experiment, H_2O_2 induced a rapid increase in $[Ca^{2+}]i$ that was blocked by pretreatment with BAPTA-AM. In contrast, A23187 induced GLUT4 translocation as early as 5 min after H_2O_2 treatment. Therefore, an H_2O_2-induced increase in $[Ca^{2+}]i$ may have resulted in the activation of both CaMKKβ and Akt. However, results obtained using BAPTA-AM and calcium ionophore should be interpreted with caution because of their potential non-specific effects. A subsequent increase in the AMP: ATP ratio may activate AMPK by direct allosteric activation and by protecting T172 from dephosphorylation, but this occurs in a later phase in cardiomyocytes with H_2O_2 stimulation.

Our results indicate that this quick response to H_2O_2 largely depends on two upstream AMP kinases and PI3-K/Akt. Since the effect of $ONOO^-$ on GLUT4 translocation in neonatal cardiac myocytes was similar to that of H_2O_2, oxidative stress may generally activate these signal transduction mechanisms. However, the signaling pathway involved in GLUT4 translocation by AMPK and PI3-K/Akt would be affected by insulin sensitivity and energy status. Further studies are needed to precisely define the signal transduction pathways that affect cardiomyocyte metabolism in response to oxidative stress.

Acknowledgments

The authors thank A. Fukumoto, N. Sowa, A. Kikukawa, and M. Nishikawa for their technical assistance. This study was

supported in part by grants (to T.K., K.H. and K.O.) from the Ministry of Education, Culture, Science, Sports, and Technology of Japan.

Literature Cited

Altarejos JY, Taniguchi M, Clanachan AS, Lopaschuk GD. 2005. Myocardial ischemia differentially regulates LKB1 and an alternate 5'-AMP-activated protein kinase kinase. J Biol Chem 280:183–190.

Anderson KA, Means RL, Huang QH, Kemp BE, Goldstein EG, Selbert MA, Edelman AM, Fremeau RT, Means AR. 1998. Components of a calmodulin-dependent protein kinase cascade. Molecular cloning, functional characterization and cellular localization of Ca^{2+}/calmodulin-dependent protein kinase kinase beta. J Biol Chem 273:31880–31889.

Baron SJ, Li J, Russell RR, Neumann D, Miller EJ, Tuerk R, Wallimann T, Hurley RL, Witters LA, Young LH. 2005. Dual mechanisms regulating AMPK kinase action in the ischemic heart. Circ Res 96:337–345.

Bogan JS, McKee AE, Lodish HF. 2001. Insulin-responsive compartments containing GLUT4 in 3T3-L1 and CHO cells: Regulation by amino acid concentrations. Mol Cell Biol 21:4785–4806.

Coven DL, Hu X, Cong L, Bergeron R, Shulman GI, Hardie DG, Young LH. 2003. Physiological role of AMP-activated protein kinase in the heart: Graded activation during exercise. Am J Physiol Endocrinol Metab 285:E629–E636.

Cushman SW, Wardzala LJ. 1980. Potential mechanism of insulin action on glucose transport in the isolated rat adipose cell. Apparent translocation of intracellular transport systems to the plasma membrane. J Biol Chem 255:4758–4762.

Fischer Y, Thomas J, Sevilla L, Munoz P, Becker C, Holman G, Kozka IJ, Palacin M, Testar X, Kammermeier H, Zorzano A. 1997. Insulin-induced recruitment of glucose transporter 4 (GLUT4) and GLUT1 in isolated rat cardiac myocytes. Evidence of the existence of different intracellular GLUT4 vesicle populations. J Biol Chem 272:7085–7092.

Goldhaber JI, Weiss JN. 1992. Oxygen free radicals and cardiac reperfusion abnormalities. Hypertension 20:118–127.

Gonzalez AA, Kumar R, Mulligan JD, Davis AJ, Saupe KW. 2004. Effects of aging on cardiac and skeletal muscle AMPK activity: Basal activity, allosteric activation, and response to in vivo hypoxemia in mice. Am J Physiol Regul Integr Comp Physiol 287:R1270–R1275.

Hardie DG, Sakamoto K. 2006. AMPK: A key sensor of fuel and energy status in skeletal muscle. Physiology (Bethesda) 21:48–60.

Hasegawa K, Meyers MB, Kitsis RN. 1997. Transcriptional coactivator p300 stimulates cell type-specific gene expression in cardiac myocytes. J Biol Chem 272:20049–20054.

Hawley SA, Boudeau J, Reid JL, Mustard KJ, Udd L, Makela TP, Alessi DR, Hardie DG. 2003. Complexes between the LKB1 tumor suppressor, STRAD alpha/beta and MO25 alpha/beta are upstream kinases in the AMP-activated protein kinase cascade. J Biol 2:28.

Hawley SA, Pan DA, Mustard KJ, Ross L, Bain J, Edelman AM, Frenguelli BG, Hardie DG. 2005. Calmodulin-dependent protein kinase kinase-beta is an alternative upstream kinase for AMP-activated protein kinase. Cell Metab 2:9–19.

Hill MM, Clark SF, Tucker DF, Birnbaum MJ, James DE, Macaulay SL. 1999. A role for protein kinase Bbeta/Akt2 in insulin-stimulated GLUT4 translocation in adipocytes. Mol Cell Biol 19:7771–7781.

Horman S, Vertommen D, Heath R, Neumann D, Mouton V, Woods A, Schlattner U, Wallimann T, Carling D, Hue L, Rider MH. 2006. Insulin antagonizes ischemia-induced Thr172 phosphorylation of AMP-activated protein kinase alpha-subunits in heart via hierarchical phosphorylation of Ser485/491. J Biol Chem 281:5335–5340.

Hurley RL, Anderson KA, Franzone JM, Kemp BE, Means AR, Witters LA. 2005. The Ca^{2+}/calmodulin-dependent protein kinase kinases are AMP-activated protein kinase kinases. J Biol Chem 280:29060–29066.

Li J, Hu X, Selvakumar P, Russell RR, Cushman SW, Holman GD, Young LH. 2004. Role of the nitric oxide pathway in AMPK-mediated glucose uptake and GLUT4 translocation in heart muscle. Am J Physiol Endocrinol Metab 287:E834–E841.

Manfredi G, Yang L, Gajewski CD, Mattiazzi M. 2002. Measurements of ATP in mammalian cells. Methods 26:317–326.

Morisco C, Condorelli G, Trimarco V, Bellis A, Marrone C, Condorelli G, Sadoshima J, Trimarco B. 2005. Akt mediates the cross-talk between beta-adrenergic and insulin receptors in neonatal cardiomyocytes. Circ Res 96:180–188.

Moyers JS, Bilan PJ, Reynet C, Kahn CR. 1996. Overexpression of Rad inhibits glucose uptake in cultured muscle and fat cells. J Biol Chem 271:23111–23116.

Ono K, Wang X, Han J. 2001. Resistance to tumor necrosis factor-induced cell death mediated by PMCA4 deficiency. Mol Cell Biol 21:8276–8288.

Sakamoto K, Zarrinpashneh E, Budas GR, Pouleur AC, Dutta A, Prescott AR, Vanoverschelde JL, Ashworth A, Jovanovic A, Alessi DR, Bertrand L. 2006. Deficiency of LKB1 in heart prevents ischemia-mediated activation of AMPKα2 but not AMPKα1. Am J Physiol Endocrinol Metab 290:E780–E788.

Sakoda T, Kasahara N, Hamamori Y, Kedes L. 1999. A high-titer lentiviral production system mediates efficient transduction of differentiated cells including beating cardiac myocytes. J Mol Cell Cardiol 31:2037–2047.

Sanders MJ, Grondin PO, Hegarty BD, Snowden MA, Carling D. 2007. Investigating the mechanism for AMP activation of the AMP-activated protein kinase cascade. Biochem J 403:139–148.

Satoh S, Nishimura H, Clark AE, Kozka IJ, Vannucci SJ, Simpson IA, Quon MJ, Cushman SW, Holman GD. 1993. Use of bismannose photolabel to elucidate insulin-regulated GLUT4 subcellular trafficking kinetics in rat adipose cells. Evidence that exocytosis is a critical site of hormone action. J Biol Chem 268:17820–17829.

Shioi T, Kang PM, Douglas PS, Hampe J, Yballe CM, Lawitts J, Cantley LC, Izumo S. 2000. The conserved phosphoinositide 3-kinase pathway determines heart size in mice. EMBO J 19:2537–2548.

Slot JW, Geuze HJ, Gigengack S, James DE, Lienhard GE. 1991. Translocation of the glucose transporter GLUT4 in cardiac myocytes of the rat. Proc Natl Acad Sci USA 88:7815–7819.

Soltys CL, Kovacic S, Dyck JR. 2006. Activation of cardiac AMP-activated protein kinase by LKB1 expression or chemical hypoxia is blunted by increased Akt activity. Am J Physiol Heart Circ Physiol 290:H2472–H2479.

Stein SC, Woods A, Jones NA, Davison MD, Carling D. 2000. The regulation of AMP-activated protein kinase by phosphorylation. Biochem J 345:437–443.

Sun D, Nguyen N, DeGrado TR, Schwaiger M, Brosius FC III. 1994. Ischemia induces translocation of the insulin-responsive glucose transporter GLUT4 to the plasma membrane of cardiac myocytes. Circulation 89:793–798.

Suzuki K, Kono T. 1980. Evidence that insulin causes translocation of glucose transport activity to the plasma membrane from an intracellular storage site. Proc Natl Acad Sci USA 77:2542–2545.

Thomas SR, Chen K, Keaney JF Jr. 2002. Hydrogen peroxide activates endothelial nitric-oxide synthase through coordinated phosphorylation and dephosphorylation via a phosphoinositide 3-kinase-dependent signaling pathway. J Biol Chem 277:6017–6024.

Tian R, Abel ED. 2001. Responses of GLUT4-deficient hearts to ischemia underscore the importance of glycolysis. Circulation 103:2961–2966.

Tian R, Musi N, D'Agostino J, Hirshman MF, Goodyear LJ. 2001. Increased adenosine monophosphate-activated protein kinase activity in rat hearts with pressure-overload hypertrophy. Circulation 104:1664–1669.

Tokumitsu H, Iwabu M, Ishikawa Y, Kobayashi R. 2001. Differential regulatory mechanism of Ca^{2+}/calmodulin-dependent protein kinase kinase isoforms. Biochemistry 40:13925–13932.

Woods A, Johnstone SR, Dickerson K, Leiper FC, Fryer LG, Neumann D, Schlattner U, Wallimann T, Carlson M, Carling D. 2003. LKB1 is the upstream kinase in the AMP-activated protein kinase cascade. Curr Biol 13:2004–2008.

Woods A, Dickerson K, Heath R, Hong SP, Momcilovic M, Johnstone SR, Carlson M, Carling D. 2005. Ca^{2+}/calmodulin-dependent protein kinase kinase-beta acts upstream of AMP-activated protein kinase in mammalian cells. Cell Metab 2:21–33.

Yamaguchi S, Katahira H, Ozawa S, Nakamichi Y, Tanaka T, Shimoyama T, Takahashi K, Yoshimoto K, Imaizumi MO, Nagamatsu S, Ishida H. 2005. Activators of AMP-activated protein kinase enhance GLUT4 translocation and its glucose transport activity in 3T3-L1 adipocytes. Am J Physiol Endocrinol Metab 289:E643–E649.

Yang J, Clark AE, Harrison R, Kozka IJ, Holman GD. 1992. Trafficking of glucose transporters in 3T3-L1 cells. Inhibition of trafficking by phenylarsine oxide implicates a slow dissociation of transporters from trafficking proteins. Biochem J 281:809–817.

Zhao J, Pettigrew GJ, Thomas J, Vandenberg JI, Delriviere L, Bolton EM, Carmichael A, Martin JL, Marber MS, Lever AM. 2002. Lentiviral vectors for delivery of genes into neonatal and adult ventricular cardiac myocytes in vitro and in vivo. Basic Res Cardiol 97:348–358.

ELSEVIER

Atherosclerosis 200 (2008) 303–309

ATHEROSCLEROSIS

www.elsevier.com/locate/atherosclerosis

Determination of LOX-1-ligand activity in mouse plasma with a chicken monoclonal antibody for ApoB

Yuko Sato[a,1], Norihisa Nishimichi[b,1], Atsushi Nakano[a,1], Kenji Takikawa[b], Nobutaka Inoue[a], Haruo Matsuda[b], Tatsuya Sawamura[a,*]

[a] *Department of Vascular Physiology, National Cardiovascular Center Research Institute, 5-7-1 Fujishirodai, Suita, Osaka 565-8565, Japan*
[b] *Laboratory of Immunobiology, Department of Molecular and Applied Biosciences, Graduate School of Biosphere Science, Hiroshima University, Hiroshima, Japan*

Received 8 August 2007; received in revised form 29 December 2007; accepted 2 February 2008
Available online 12 February 2008

Abstract

Oxidized LDL (OxLDL) is implicated in endothelial dysfunction as well as the formation and progression of atherosclerosis. It has become evident that the atherogenic properties induced by OxLDL are mainly mediated via lectin-like OxLDL receptor-1 (LOX-1). Over the past decade, much research has been performed to investigate lipid metabolism and atherogenesis using genetically engineered mice. To understand the significance of OxLDL, methods to measure the levels of OxLDL in these experimental animals should be established. Utilizing a chicken monoclonal antibody technique, here, we generated anti-human ApoB antibodies that are able to recognize mouse VLDL/LDL. These antibodies were selected from single chain fragment of variable region (scFv) phage library constructed from chickens immunized with human LDL. One of these antibodies, HUC20, was reconstructed into IgY form. Immunohistochemical analysis revealed that this novel antibody specifically stains atherosclerotic lesions of ApoE-deficient mice, associated with Oil red O positive and macrophage-antigen-positive regions.

Furthermore, in combination with recombinant LOX-1, a sandwich enzyme immunoassay was developed to measure the levels of LOX-1 ligands in mouse plasma. The sandwich enzyme immunoassay revealed a dramatic increase in the level of LOX-1 ligands in the plasma of ApoE-deficient mice fed high-fat diet, suggesting a link between the level of LOX-1-ligands and the progression of atherosclerosis in mice. Hence, the chicken anti-ApoB monoclonal antibody HUC20 developed here, could be a useful tool to analyze the role of ApoB-containing lipoprotein in atherogenesis in mice.

Keywords: LOX-1; Oxidized LDL; Mouse apolipoprotein B; Atherosclerosis

1. Introduction

Oxidatively modified low-density lipoprotein (LDL) has been implicated in endothelial dysfunction as well as the progression of atherosclerosis [1–3]. In response to stimulation of oxidized LDL (OxLDL), the production of nitric oxide is impaired and expression of chemoattractants for monocytes, leukocyte adhesion molecules, and growth factors for smooth muscle cells are induced in endothelial cells. These cellular events contribute to the formation of atherosclerotic lesions. Lectin-like OxLDL receptor-1 (LOX-1) was originally identified as a receptor for OxLDL expressed in vascular endothelial cells [4], and it has become evident that these atherogenic events induced by OxLDL are mainly mediated via LOX-1. Furthermore, we demonstrated significant *in vivo* roles of LOX-1 using genetically modified mice. Recently, we showed that deletion of LOX-1 in LDLR knockout (KO) mice led to a reduction in atherogenesis in association with a reduction in proinflammatory and pro-oxidant signals [5]. On the other hand, mice overexpressing LOX-1 in coronary vessels and cardiomyocytes showed accumulation of

* Corresponding author. Tel.: +81 6 6833 5012x2518; fax: +81 6 6835 5329.
E-mail address: t-sawamura@umin.ac.jp (T. Sawamura).
[1] These authors contributed equally.

0021-9150/$ – see front matter © 2008 Elsevier Ireland Ltd. All rights reserved.
doi:10.1016/j.atherosclerosis.2008.02.001

OxLDL in coronary arteries and inflammatory vasculopathy in a hyperlipidemic mouse model [6]. Thus, there is accumulating evidence that the interaction of OxLDL with LOX-1 plays an essential role in endothelial activation and/or dysfunction in atherosclerosis.

Over the last decade, progress in research on lipoprotein metabolism and atherosclerosis has been achieved by extensive investigations using genetically engineered mice. For example, a great deal of research breakthroughs has been made using ApoE or LDL receptor KO to clarify the pathogenesis of atherosclerosis-based cardiovascular diseases and lipid disorder, since atherogenesis in these experimental mice share many characteristics with human atherosclerotic lesions. To understand the underlying mechanisms, it is important to reveal a causal linkage between not only the plasma levels of lipoproteins, but also the accumulation of OxLDL and the pathogenesis of atherosclerosis; therefore, a specific assay for OxLDL in rabbits was developed and the direct relationship between OxLDL and atherogenesis was demonstrated [7,8]. However, there has been no tool to evaluate the interaction between LOX-1 and LOX-1 ligands such as OxLDL in mice until now. Indeed, mice monoclonal antibodies against mice ApoB-100 or ApoB-48 were previously generated, but these mice antibodies are not suitable for immunohistochemical study because of cross-reactivity of the secondary antibody for endogenous immunoglobulin.

In some cases, it is difficult to use mammals to create antibodies for biomolecules that have attained high levels of conservation in mammals. However, even in such cases, the target antibodies can be made with ease by having bird species develop immunity against the molecules. In the present study, we generated a chicken monoclonal antibody against mouse ApoB-containing lipoproteins. Furthermore, we developed a novel sandwich enzyme immunoassay for LOX-1 ligands in mouse plasma by applying this novel antibody and recombinant LOX-1. Using this method, we investigated the linkage between LOX-1 ligand activity and the atherogenesis in mice.

2. Methods

2.1. Chicken and immunization

Three 1-month-old H-B15 inbred chickens were immunized intraperitoneally (i.p.) with 100 μg of human LDL (Chemicon, Temecula, CA) together with an equal amount of alum solution. The animals received three additional intraperitoneal injections of the corresponding antigen at 3-week intervals.

2.2. Selection of scFv phage displayed antibody

Three days after the final injection, spleen cells were isolated from immunized chickens. The RNA extraction from spleen cells, amplification of immunoglobulin variable region (V_H and V_L) genes and construction of scFv phage library were performed by methods described previously [9]. The scFv phage clones were selected by panning method using Nunc-Immuno Module (Nunc, Roskilde, Denmark) coated with human LDL. For selection of the specific phage clones, Nunc-Immuno Module was coated with 100 μl of 5 μg/ml human LDL, human ApoB (Chemicon), mouse VLDL/LDL and mouse HDL, respectively, at 4 °C overnight. The plates were then blocked with phosphate buffered saline (PBS) containing 20% (w/v) ImmunoBlock (DS Pharma, Osaka, Japan) at 4 °C overnight. One hundred μl of phage solution was added to each well and the plates were incubated at 37 °C for 1 h. After washing, 100 μl of peroxidase-conjugated anti-chicken Ig-Fab fragment antibody (Bethyl laboratories, Montgomery, TX) diluted with PBS containing 5% (w/v) ImmunoBlock was added to each well and the plates were incubated at 37 °C for 1 h. After five washings, 100 μl of *o*-phenylenediamine sulfate (Sigma Chemical, St. Louis, MO) was added and their optical density was measured at 490 nm.

2.3. Preparation of recombinant IgY

For construction of recombinant IgY (rIgY), heavy chain and light chain expression vectors [10] were used, with the exception that cloning of heavy and light chain leader sequences were amplified from genome DNA from the HUC2-13 chicken hybridoma cells [11]. Approximately 6×10^7 FreeStyle 293-F cells (Invitrogen, Carlsbad, CA) were co-transfected by lipofection with a total of 80 μg of constructed VH and VL plasmid DNA for rIgY expression. After 72 h of transfection, the rIgY was purified from the supernatants by a ProBond Resin purification system (Invitrogen). Purified rIgY was dialyzed against PBS, and concentration of the rIgY was measured using a BCA Protein Assay kit (Pierce Biotechnology, Rockford, IL). The specificity of the purified rIgY was examined by enzyme-linked immunosorbent assay (ELISA) and Western blotting analyses. The dinitrophenyl (DNP)-specific rIgY, B4 [12], was used as a control rIgY.

2.4. Preparation of recombinant LOX-1

cDNA encoding the extracellular domain of human LOX-1 was subcloned into pcDNA4 with chicken IgG light chain leader peptide and 6× His tag in *N*-terminus. FreeStyle 293-F cells (Invitrogen) were transiently transfected with the expression vector. Four days after transfection, the recombinant LOX1 was purified from the culture supernatant with Ni-NTA superflow (Qiagen, Germantown, MD) according to the manufacturer's instruction.

2.5. Sandwich ELISA for LOX-1 ligand activity

Recombinant LOX-1 (0.4 μg/well) was immobilized on 96-well plates (Maxisorp, Nunc) by incubating overnight at 4 °C in 50 μl of PBS. After two washes with PBS, the plates were blocked with 0.3 ml of 20% (v/v) ImmunoBlock (DS

Pharma) for 8 h at 4 °C. After three washes with PBS, the plates were incubated with 0.1 ml of the standard OxLDL or plasma diluted 40 times with EDTA–HEPES buffer [10 mM HEPES (pH 7.0), 150 mM NaCl, 2 mM EDTA]. Then, the plates were washed three times with PBS, and incubated for 1 h at room temperature with 0.5 μg/ml HUC20 in PBS containing 1% (w/v) BSA. After three washes with PBS, the plates were incubated for 1 h at room temperature with the peroxidase-conjugated goat anti-chicken IgG (H + L) (KPL, Gaithersburg, MD) diluted 2000 times with PBS containing 1% (w/v) BSA. After five washes with PBS, the substrate solution containing 3,3′,5,5′-tetramethylbenzidine (TMB solution, Bio-Rad Laboratories, Hercules, CA) was added to the plates and incubated at room temperature for 30 min. The reaction was terminated with 50 μl of 2 M sulfuric acid. Peroxidase activity was determined by measurement of absorbance at 450 nm.

3. Results

3.1. Isolation of phage clones that recognize both human and mouse ApoB

To obtain the antibodies against ApoB with broader interspecies cross-reactivity, we immunized chicken with human LDL. After immunization five times, a phage display library was constructed from splenocytes of the chickens that express the immunoglobulin variable region. After the fifth round of panning selection of the phages, the specificity of the concentrated phage library was examined by ELISA using human LDL, human ApoB, mouse VLDL/LDL, and mouse HDL. The condensed library reacted with human LDL, human ApoB and mouse VLDL/LDL, but not with mouse HDL (data not shown). Thirteen independent scFv clones were isolated from the condensed library. Among them, seven clones were cross-reactive with mouse VLDL/LDL (Fig. 1A), indicating that these antibodies recognize ApoB as common molecule between human ApoB and mouse VLDL/LDL.

3.2. Construction of recombinant IgY

One of the seven scFv antibodies recognizing both human and mouse ApoB, #20, was reconstructed into IgY form containing a histidine tag in the C-terminal and named as HUC20. The HUC20 IgY from 293-F cells was purified from the supernatant by nickel affinity resin. The purified HUC20 was detected as a single band (250 kDa) in SDS-PAGE under non-reducing condition and the band was also detectable by Western blot analysis using anti-chicken IgG antibody (data not shown).

The reactivity of the HUC20 as assessed by ELISA showed that HUC20 was reactive with human LDL, human ApoB, and mouse VLDL/LDL, but not with mouse HDL (Fig. 1B). The results of the HUC20 reactivity reproduced that of the original #20 scFv phage-antibody. In contrast,

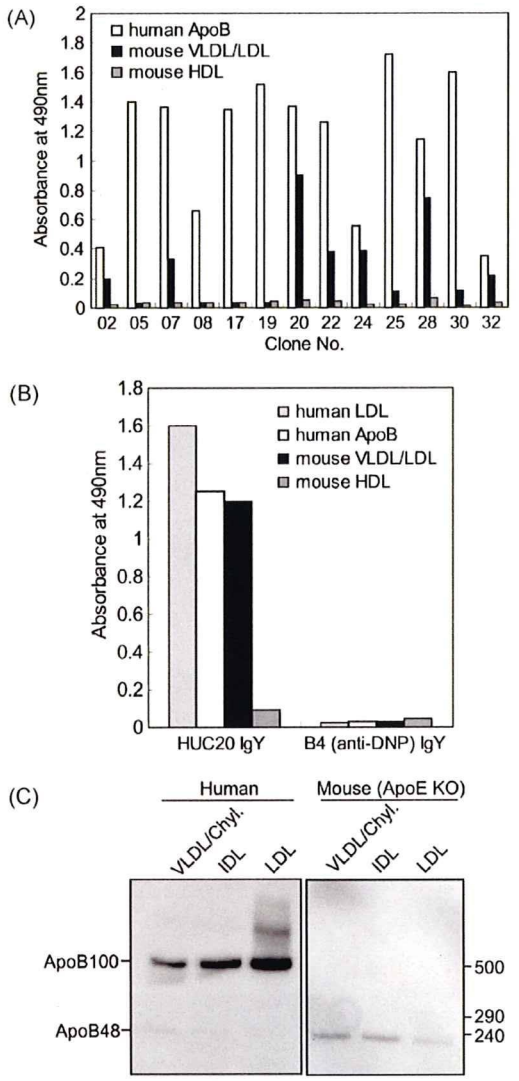

Fig. 1. Isolation of the antibody against human and mouse ApoB. (A) ELISA reactivity of scFv clones against human ApoB, mouse VLDL/LDL and mouse HDL, respectively. (B) ELISA reactivity of HUC20 rIgY against human LDL, human ApoB, mouse VLDL/LDL and mouse HDL. B4 rIgY was used as a negative control. (C) Western blotting analysis of lipoproteins with HUC20. Plasma from human and mouse (ApoE KO) was separated by sequential ultracentrifugation. Lipoproteins (100 ng) of each fraction were separated by SDS-PAGE followed by Western blotting with HUC20. HUC20 recognized ApoB-48 (approximately 240 kDa) as well as ApoB-100 (approximately 500 kDa).

a control rIgY, B4, reacted with none of the above antigens. To further investigate the recognition of HUC20, Western blotting analysis of lipoproteins from human and mouse (ApoE KO) plasma was performed. As shown in Fig. 1C, HUC20 recognized ApoB-100 (approximately 500 kDa) in VLDL/chylomicron, IDL, and LDL fractions from human as well as ApoB-48 (approximately 240 kDa) in VLDL/chylomicron from human. HUC20 also recognized ApoB-48 in VLDL/chylomicron, IDL, and LDL fractions from ApoE KO mice, in which plasma, ApoB-48-containing lipoproteins were highly accumulated [13]. Thus, HUC20

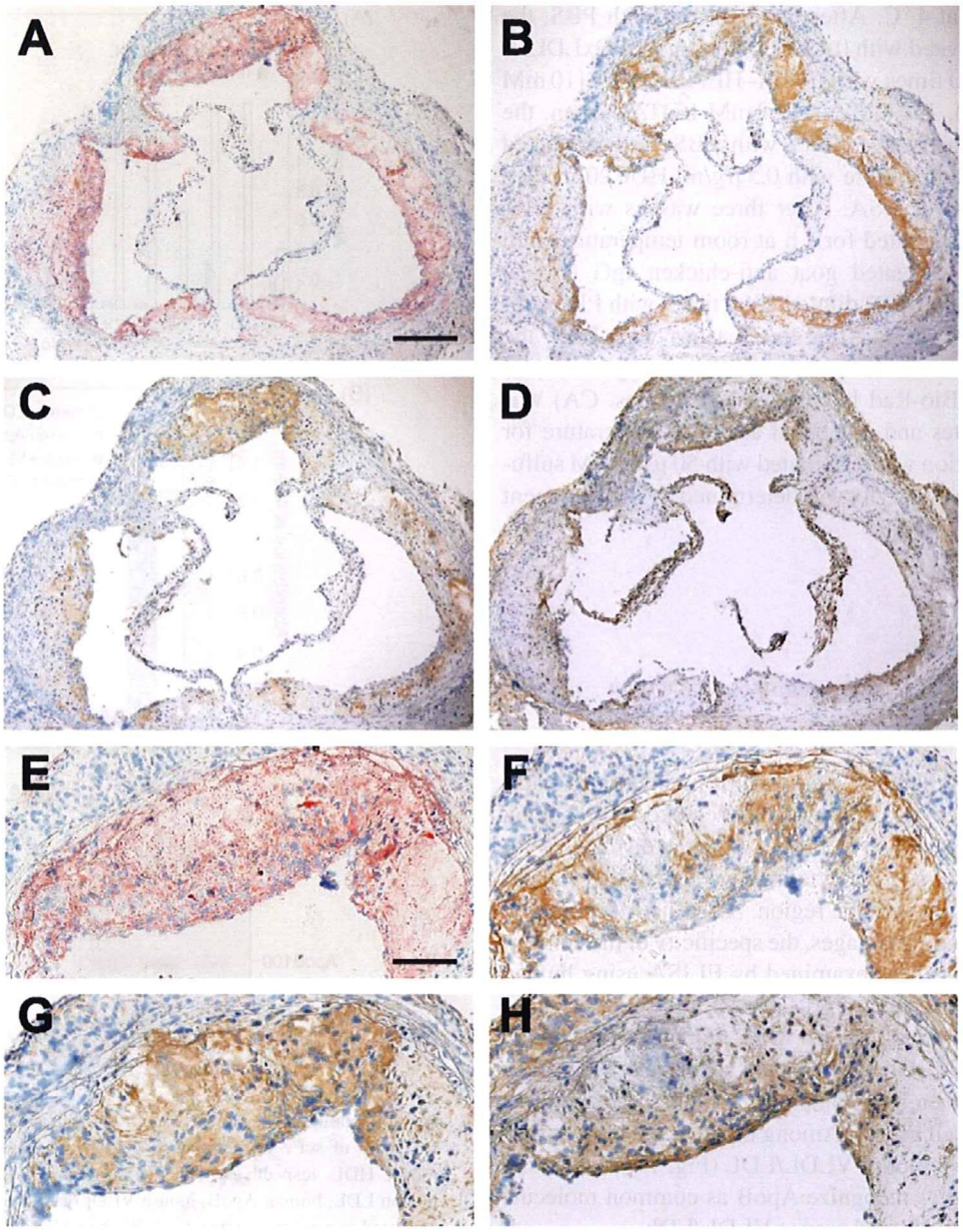

Fig. 2. Immunohistochemical detection of ApoB and LOX-1 ligand in atheroma. Sections of aortic root of 24-week-old ApoE KO mice stained with (A) Oil red O, (B) HUC20, (C) anti-macrophage antibody, (D) recombinant LOX-1 and (E)–(H) magnified view of A–D, respectively. Bars = 200 μm (A)–(D) and 100 μm (E)–(H).

recognizes both ApoB-100 and ApoB-48-containing lipoproteins.

3.3. Immunohistochemical detection of ApoB and LOX-1 ligand in atheroma

Utilizing HUC20, we performed immunohistochemical analyses of atheroma in aortic root of ApoE KO mice fed HF (high fat) diet. The ApoB-like immunoreactivity detected by HUC20 (Fig. 2B and F) was well co-localized with the lipid deposits detected by the Oil red O staining (Fig. 2A and E), where macrophage-derived foam cells were accumulated (Fig. 2C and G). These findings are in good agreement with the results from other species including human [14,15].

We further characterized mouse atheroma by the use of recombinant LOX-1 to detect LOX-1 ligand-like activity in these lesions, which is postulated to recognize oxidatively modified lipoproteins. As shown in Fig. 2D and H, the lesions associated with intimal thickening were positive for LOX-1 ligand activity. The existence of both ApoB-like immunoreactivity and LOX-1 ligand-like activity in atheromatous lesions suggests that these lesions might contain ApoB-containing oxidatively modified lipoproteins.

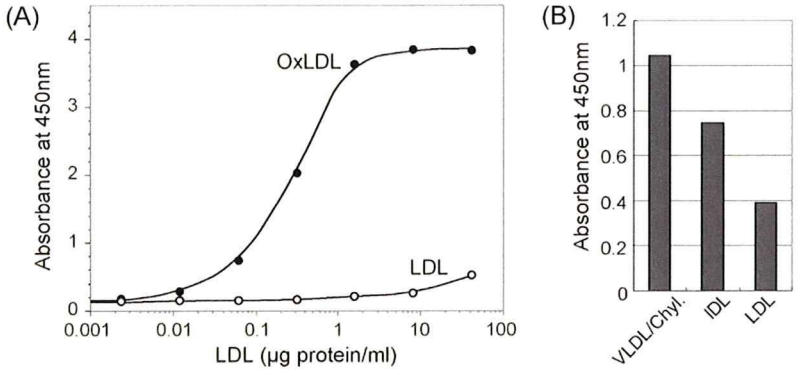

Fig. 3. Determination of LOX-1 ligand activity in human plasma. (A) Specificity of our ELISA system for modified LDL. The reactivity to OxLDL (filled circles) and LDL (open circles). (B) Reactivity of lipoproteins to LOX-1. Lipoproteins (10 μg protein/ml) isolated by sequential ultracentrifugation from human plasma were subjected to sandwich ELISA assay with LOX-1 and HUC20. Each fraction of lipoprotein reacted with LOX-1. The order of reactivity of LOX-1 was as follows: VLDL/chylomicron > IDL > LDL.

Table 1
Hemodynamic and plasma lipid indices

	WT control diet	WT HF diet	ApoE KO control diet	ApoE KO HF diet
Body weight (g)	23.9 ± 0.4	23.2 ± 0.2	22.6 ± 0.7	22.7 ± 1.1
SBP (mmHg)	113.7 ± 3.2	113.4 ± 3.8	109.9 ± 3.8	110.4 ± 4.8
MBP (mmHg)	82.2 ± 2.2	82.4 ± 4.1	77.8 ± 7.2	79.4 ± 3.4
DBP (mmHg	66.7 ± 2.1	66.8 ± 4.6	61.9 ± 2.2	64.2 ± 2.9
Heart rate (BPM)	535.0 ± 18.6	637.4 ± 21.1	536.9 ± 26.5	579.8 ± 15.7
Total cholesterol (mg/dl)	74.2 ± 4.2	191.4 ± 9.7	479.2 ± 40.2	3189.0 ± 162.5
Phospholipid (mg/dl)	165.3 ± 4.7	194.2 ± 11.0	315.4 ± 22.2	882.9 ± 42.4
Triglyceride (mg/dl)	53.9 ± 6.3	46.2 ± 6.7	136.7 ± 14.9	110.3 ± 4.8
HDL (mg/dl)	52.8 ± 2.1	39.4 ± 4.10	12.0 ± 2.5	14.1 ± 4.6

Data were collected at 9 weeks of age. Each animal ($n = 8$) fed control diet and after 2-week high-fat (HF) diet. SBP indicates systolic blood pressure; MBP, mean blood pressure; DBP, diastolic blood pressure. Values are expressed as the mean ± S.E.M.

3.4. Detection of LOX-1 ligand activity in the plasma of human and ApoE KO mice

Combining the specificity of HUC20 for ApoB-containing lipoprotein and affinity of recombinant LOX-1 for OxLDL, we developed a sandwich ELISA system and applied it to quantify LOX-1 ligand activity in mouse plasma. This sandwich ELISA detected OxLDL as low as 1 ng/ml, but not native LDL even at the concentration of 10 μg/ml (Fig. 3A). Furthermore, we examined the characterization of the LOX-1 ligand lipoproteins in plasma. For the purpose, lipoprotein fractions (VLDL/chylomicron, IDL, and LDL) isolated by sequential ultracentrifugation from pooled plasma of human were subjected to sandwich ELISA assay with LOX-1 and HUC20. As shown in Fig. 3B, LOX-1 recognizes each fraction of lipoprotein. The order of reactivity of LOX-1 was as follows: VLDL/chylomicron > IDL > LDL.

Next, using this sandwich ELISA system, the alterations of the plasma levels of LOX-1 ligand activity in mice model of atherosclerosis were evaluated. We measured the plasma levels of LOX-1 ligand activity from wild type- or ApoE KO-mice fed normal or HF diet. LOX-1 ligand activity in the plasma of WT and ApoE KO mice fed normal diet was 5 ± 1 ng/ml and 30 ± 3 ng/ml, respectively. As shown in Table 1, HF diet significantly increased plasma cholesterol level in both wild type- and ApoE KO-mice. Concomitantly, LOX-1 ligand activities in the plasma of WT and ApoE KO mice were elevated as 71 ± 13 ng/ml and 1145 ± 115 ng/ml, respectively (Fig. 4A). The dilution curve of the plasma from ApoE KO mouse fed HF diet was accurately plotted on the line of standard curve of OxLDL, suggesting the plasma concentration of LOX-1 ligand is estimated well by reference to OxLDL (Fig. 4B).

4. Discussion

In this study we generated a novel chicken monoclonal antibody, HUC20, that recognizes mouse ApoB as well as that of human. The reactivity of HUC20 is specific and sensitive enough to detect mouse ApoB-containing lipoproteins in tissue by immunohistochemistry and those in plasma by enzyme immunoassay. Further, this sandwich enzyme immunoassay for LOX-1 ligands, which we developed by combining HUC20 and recombinant LOX-1, is sensitive enough to detect the increase of ApoB-containing LOX-1-ligands in mice fed a HF diet.

Well-known coronary risk factors such as hyperlipidemia, hypertension, diabetes, and metabolic syndrome induce oxidative stress. Under enhanced oxidative stress, the lipids

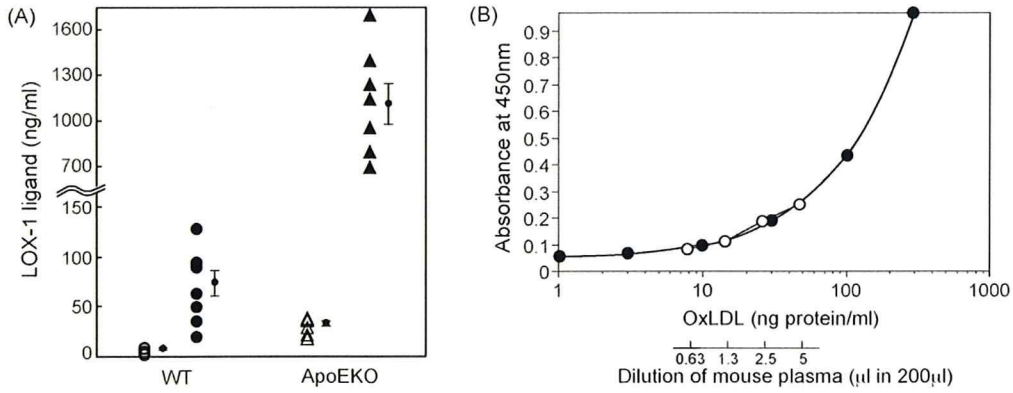

Fig. 4. Determination of LOX-1 ligand activity in plasma of ApoE KO mice. (A) Individual plasma LOX-1 ligand levels in WT mice fed control diet and HF diet (open and filled circles) and ApoE KO mice fed control and HF diet (open and filled triangles). Each bar represents the mean ± S.E.M., $n = 8$. (B) ELISA calibration curve for OxLDL in assay buffer (filled circles) and comparison with dilution curve for ApoE KO (2-week high-fat diet) plasma sample (open circles).

retained in the arterial wall are susceptible to oxidative modification. The oxidized lipids formed induce vascular inflammation, which, in turn, promotes the process of atherosclerosis. Among the oxidized lipids, OxLDL plays a crucial role in the pathogenesis of atherosclerosis. Various biomarkers have been proposed to evaluate the redox state and the plasma levels of OxLDL, such as isopentanes, 8-hydroxy-2′-deoxyguanine. Previous epidemiological studies demonstrated that level of OxLDL is a potent risk factor for the onset of coronary artery diseases, even if the levels of cholesterol are within the normal range. Indeed, Ehara et al. demonstrated that the levels of OxLDL in patients with acute coronary syndrome were much higher than stable angina [16]. However, more direct linkage between the LDL oxidation and the progression of atherosclerosis has been vague in genetically engineered mice such as ApoE or LDL receptor KO mice, because of the lack of a specific assay for OxLDL in mouse plasma.

Chickens are useful for the acquisition of specific antibodies against proteins conserved among mammalian species. In the case of ApoB, the homology of ApoB-48 between human and mice is 78%, whereas that between human and chicken is 48%. Thus, it is difficult to raise specific antibodies against such conserved proteins like apoproteins. Using the chicken we can overcome such problems. Further, by the application of recombinant DNA technology using scFv phages, we can choose a single clone that is specific, sensitive, and suitable for particular use as an antibody. The chicken monoclonal antibody system has a merit in that scalable production is possible, as is common in monoclonal antibodies raised from other species. Another advantage of a chicken monoclonal antibody raised against the mouse is the ease of application to study in the mouse. Mouse antibodies are often unsuitable for investigation of mice themselves, because the secondary antibody against mouse immunoglobulin recognizes endogenous mouse immunoglobulin.

When considering the possibilities of raising genetically engineered mice as models for human diseases, including hyperlipidemia and atherosclerosis, it is crucial to develop and use analytical methods applicable to both human and mouse in order to understand disease and develop therapeutic strategies. Despite a common recognition for the importance of ApoB-containing lipoproteins and their oxidized form in the pathogenesis of atherosclerosis, immunological tools to dissect the problem in mice have not been well established. Here we successfully developed a chicken monoclonal antibody for ApoB and an ELISA system to determine ApoB-containing LOX-1 ligand, which can be applied for both human and mouse studies. These will give us the opportunity to analyze the precise roles of ApoB-containing lipoproteins and their oxidized form in various disease.

LOX-1 mediates endothelial dysfunction induced by chylomicron/remnants as well as modified LDL [17,18]. Therefore, the combination of recombinant LOX-1 and HUC20 which recognizes both ApoB-48 and ApoB-100, could detect atherogenic ApoB-containing lipoproteins in both VLDL/LDL and chylomicron/remnants fractions by the present ELISA system. HUC20 might also be needed for a certain tool for the detection of ApoB-48 in atherosclerosis lesions.

Indeed in the present study, we showed the accumulation of ApoB-containing lipoproteins and LOX-1 ligand in atheroma. We also found that LOX-1 ligand activity was significantly elevated in the plasma of ApoE KO mice fed HF diet. Furthermore, removal of LOX-1 ligands from plasma by the ectopic expression of LOX-1 in mouse liver significantly suppressed the progression of atherosclerosis (Katagiri H, unpublished data). As well known, ApoE KO mice show significant increase in HF diet of VLDL and chylomicron/remnants rather than LDL. Therefore, it should be noted that LOX-1 ligand activity we measured in this mice model might reflect the activity in the fractions of VLDL and chylomicron/remnants. In any case, the data suggest that the accumulation of ApoB-containing LOX-1 ligands might enhance the progression of atherosclerosis in mice, and LOX-1 ligand level would also be an important indicator for the

diagnosis and the evaluation of atherosclerosis and ischemic heart diseases in the genetically modified mouse model and in humans.

In summary, we generated a chicken monoclonal antibody HUC20 that recognizes both mouse and human ApoB, which can detect LDL in mouse atheroma. Furthermore, we developed an ELISA assay for OxLDL/VLDL that measures ApoB-containing LOX-1 ligands. This antibody will be a useful tool for research with regard to dyslipidemia, atherosclerosis, and ischemic heart diseases.

References

[1] Witztum JL, Steinberg D. Role of oxidized low density lipoprotein in atherogenesis. J Clin Invest 1991;88:1785–92.

[2] Ross R. The pathogenesis of atherosclerosis: a perspective for the 1990s. Nature 1993;362:801–9.

[3] Steinberg D. Low density lipoprotein oxidation and its pathobiological significance. J Biol Chem 1997;272:20963–6.

[4] Sawamura T, Kume N, Aoyama T, et al. An endothelial receptor for oxidized low-density lipoprotein. Nature 1997;386:73–7.

[5] Mehta JL, Sanada N, Hu CP, et al. Deletion of LOX-1 reduces atherogenesis in LDLR knockout mice fed high cholesterol diet. Circ Res 2007;100:1634–42.

[6] Inoue K, Arai Y, Kurihara H, Kita T, Sawamura T. Overexpression of lectin-like oxidized low-density lipoprotein receptor-1 induces intramyocardial vasculopathy in apolipoprotein E-null mice. Circ Res 2005;97:176–84.

[7] Kakutani M, Ueda M, Naruko T, Masaki T, Sawamura T. Accumulation of LOX-1 ligand in plasma and atherosclerotic lesions of Watanabe heritable hyperlipidemic rabbits: identification by a novel enzyme immunoassay. Biochem Biophys Res Commun 2001;282:180–5.

[8] Oka K, Yasuhara M, Suzumura K, Tanaka K, Sawamura T. Antioxidants suppress plasma levels of lectinlike oxidized low-density lipoprotein receptor-ligands and reduce atherosclerosis in watanabe heritable hyperlipidemic rabbits. J Cardiovasc Pharmacol 2006;48:177–83.

[9] Nakamura N, Shimokawa M, Miyamoto K, et al. Two expression vectors for the phage-displayed chicken monoclonal antibody. J Immunol Methods 2003;280:157–64.

[10] Shimamoto T, Nishibori N, Aosasa M, et al. Stable production of recombinant chicken antibody in CHO-K1 cell line. Biologicals 2005;33:169–74.

[11] Matsuda H, Mitsuda H, Nakamura N, et al. A chicken monoclonal antibody with specificity for the N-terminal of human prion protein. FEMS Immunol Med Microbiol 1999;23:189–94.

[12] Miyamoto K, Kimura S, Nakamura N, et al. Chicken antibody against a restrictive epitope of prion protein distinguishes normal and abnormal prion proteins. Biologicals 2007.

[13] Zhang SH, Reddick RL, Piedrahita JA, Maeda N. Spontaneous hypercholesterolemia and arterial lesions in mice lacking apolipoprotein E. Science 1992;258:468–71.

[14] Chen M, Kakutani M, Minami M, et al. Increased expression of lectin-like oxidized low density lipoprotein receptor-1 in initial atherosclerotic lesions of Watanabe heritable hyperlipidemic rabbits. Arterioscler Thromb Vasc Biol 2000;20:1107–15.

[15] Olofsson SO, Boren J. Apolipoprotein B: a clinically important apolipoprotein which assembles atherogenic lipoproteins and promotes the development of atherosclerosis. J Intern Med 2005;258:395–410.

[16] Ehara S, Ueda M, Naruko T, et al. Elevated levels of oxidized low density lipoprotein show a positive relationship with the severity of acute coronary syndromes. Circulation 2001;103:1955–60.

[17] Shin HK, Kim YK, Kim KY, Lee JH, Hong KW. Remnant lipoprotein particles induce apoptosis in endothelial cells by NAD(P)H oxidase-mediated production of superoxide and cytokines via lectin-like oxidized low-density lipoprotein receptor-1 activation: prevention by cilostazol. Circulation 2004;109:1022–8.

[18] Park SY, Lee JH, Kim YK, et al. Cilostazol prevents remnant lipoprotein particle-induced monocyte adhesion to endothelial cells by suppression of adhesion molecules and monocyte chemoattractant protein-1 expression via lectin-like receptor for oxidized low-density lipoprotein receptor activation. J Pharmacol Exp Ther 2005;312:1241–8.

Endothelium, 15:137–141, 2008

ISSN: 1062-3329 print/1543-5261 online
DOI: 10.1080/10623320802125433

informa
healthcare

Essential Role of NOXA1 in Generation of Reactive Oxygen Species Induced by Oxidized Low-Density Lipoprotein in Human Vascular Endothelial Cells

Tomoyuki Honjo, Kazunori Otsui, Rio Shiraki, and Seinosuke Kawashima
Division of Cardiovascular and Respiratory Medicine, Department of Internal Medicine, Kobe University Graduate School of Medicine, Kobe, Japan

Tatsuya Sawamura
Department of Vascular Physiology, National Cardiovascular Center Research Institute, Osaka, Japan

Mitsuhiro Yokoyama
Division of Cardiovascular and Respiratory Medicine, Department of Internal Medicine, Kobe University Graduate School of Medicine, Kobe, Japan

Nobutaka Inoue
Department of Vascular Physiology, National Cardiovascular Center Research Institute, Osaka, Japan

Oxidative stress induced by superoxide plays an important role in pathogenesis of cardiovascular diseases. NAD(P)H oxidase is a principal enzymatic origin for superoxide in vasculature. Recently, novel homologues of cytosolic components of NAD(P)H oxidase, Nox organizer 1 (NOXO1) and Nox activator 1 (NOXA1), are identified. On the other hand, oxidized low-density lipoprotein (ox-LDL) generates reactive oxygen species (ROS) in endothelial cells via lectin-like oxidized low-density lipoprotein receptor-1 (LOX-1). In the present investigation, the authors examined the expression, the regulation, and the role of NOXA1 in the generation of ROS in endothelial cells. The expression of NOXA1 was confirmed by reverse transcriptase–polymerase chain reaction (RT-PCR). Dihydroethidium method showed that ox-LDL and angiotensin II increased the generation of intracellular ROS. Once the expression of $p22^{phox}$ or NOXA1 was suppressed by siRNA, the generation of ROS induced by ox-LDL and angiotensin II were potently decreased. Moreover, the expression of NOXA1 was increased by ox-LDL in a time- and dose-dependent manner. In conclusion, endothelial NOXA1 plays an essential role in generation of ROS. Ox-LDL not only increased the generation of ROS via LOX-1, but also enhanced the expression of NOXA1 in endothelial cells. NOXA1 is likely a key player that links ox-LDL with the activation of endothelial NAD(P)H oxidase.

Keywords Endothelium, NAD(P)H Oxidase, Oxidized LDL, $p22^{phox}$, ROS

Received 8 January 2008; accepted 25 March 2008.
Address correspondence to Nobutaka Inoue, MD, PhD, Department of Vascular Physiology, National Cardiovascular Center Research Institute, 5-7-1, Fujishirodai, Suita, Osaka, 565-8565, Japan. E-mail: nobutaka@ri.ncvc.go.jp

Oxidative stress induced by superoxide in vasculature plays an in important role in pathogenesis of various cardiovascular diseases, including atherosclerosis, hypertension, ischemia-reperfusion injury, and vascular remodeling. To date, various enzymatic origins for reactive oxygen species (ROS) in the vasculature have been proposed, including xanthine oxidase, myeloperoxidase, lipoxygenase, and NAD(P)H oxidase. Among these, NAD(P)H oxidase is the most important origin of ROS in human coronary arteries (Kobayashi et al. 2003; Azumi et al. 2002). NAD(P)H oxidase was originally identified as a principal enzymatic origin in phagocytes, and this phagocyte NAD(P)H oxidase is located on a very front line in host-defense system. The phagocyte NAD(P)H oxidase is dormant in resting cells, but becomes activated to produce superoxide, a precursor of microbicidal oxidants, by interacting with the adaptor proteins $p47^{phox}$ and $p67^{phox}$ as well as the small GTPase Rac. Griendling et al. reported that vascular cells such as vascular smooth muscle cells and endothelial cells possess the activity to generate ROS in a NADH- and NADPH-dependent manner (Griendling et al. 1994). Progress in this field has revealed the molecular identification of nonphagocytic NAD(P)H oxidase in the past few years. Besides the components of phagocyte NAD(P)H oxidase, several protein homologs to $gp91^{phox}$/Nox2 were identified (the Nox family oxidases) (Lambeth 2004; Geiszt and Leto 2004). Recently, homologs of $p47^{phox}$ and $p67^{phox}$ were reported and shown to be required for activation of Nox1. The $p47^{phox}$ homolog is named as NOXO1 (NOX organizer 1), whereas the $p67^{phox}$ homolog is named as NOXA1 (NOX activator 1) (Banfi et al. 2003; Geiszt et al. 2003; Takeya et al. 2003; Takeya and

Sumimoto 2003). However, their functional roles in the activation of vascular NAD(P)H oxidase remains to be elucidated.

Clinical investigations have demonstrated that well-known coronary risk factors such as diabetes, hyperlipidemia, hypertension, smoking, and metabolic syndrome are associated with oxidative stress. Under the oxidative stress, low-density lipoprotein (LDL) particle, which are trapped in the vessel wall, are oxidative modified. Formed oxidized low-density lipoprotein (ox-LDL) is a potent inducer of endothelial injury with associated its dysfunction. ox-LDL induces the inflammatory responses, including the up-regulation of adhesion molecules, cytokines, and chemotactic factors. These cellular events are mediated via lectin-like oxidized low-density lipoprotein receptor-1 (LOX-1)–mediated pathway. LOX-1, a multiligand receptor, was originally identified as the major ox-LDL receptor in endothelial cells (Sawamura et al. 1997). The expression of LOX-1 in endothelial cells is markedly increased in vitro by cytokines and also is induced in vivo in hypertension, diabetes, and hyperlipidemia in animal models (Li et al. 2004; Nagase et al. 2000; Chen et al. 2000). Ligand binding to LOX-1 induces superoxide generation, which is accompanied by reduction of nitric oxide in endothelial cells (Cominacini et al. 2001). The activation of LOX-1 by ox-LDL induced the generation of ROS via NAD(P)H oxidase. We previously demonstrated that the NAD(P)H oxidase is expressed in coronary arteries of patients with ischemica heart disease (Kobayashi et al. 2003; Azumi et al. 2002). Further, LOX-1 is up-regulated in atherosclerotic lesions (Chen et al. 2000; Kataoka et al. 1999). Therefore, the clarification of the interaction of NAD(P)H oxidase and LOX-1 provides a new insight into understanding the pathogenesis of atherosclerosis-based ischemic heart diseases. In this study, we investigated the functional roles of NOXA1 in regulation of endothelial NAD(P)H oxidase and its interaction of LOX-1.

MATERIALS AND METHODS

Cell Culture

EAhy926, a continuous human umbilical vein endothelial cells line, was cultured in Dulbecco's modified Eagle's medium (Sigma Chemical, St. Louis, MO, USA) with 10% fetal bovine serum (JRH Biosciences, Lenexa, KS, USA), and with 100 IU/mL antibiotic-antimyotic.

Preparation of Oxidized Lipoprotein

LDL was isolated by sequential ultracentrifugation from healthy human plasma, as described previously (Sawamura et al. 1997). LDL was oxidatively modified by exposing to 7.5 mol/L $CuSO_4$ for 16 h at 37°C at the protein concentration of 3 mg/mL in phosphate-buffered saline. The degree of oxidation was estimated by measuring the amount of thiobarbituric acid-reactive substances (TBARS) and the relative electrophoretic mobility (REM) in agarose gel compared with native LDL.

Small Interfering RNA

NOXA1 and $p22^{phox}$ expression were inhibited by the Stealth small interfering RNA (RNAi) (Invitrogen, CA, USA). The siRNA target sequences were as follows: 5′-GGGCATTTGACC AAGCCGTGACCAA-3′ and 5′-GCCATTGCGAGCGGCATC TACCTAC-3′, respectively. EAhy926 were transfected with Stealth RNAi at a final concentration of 250 nmol/L by the use of oligofectamine reagent (Invitrogen). The Stealth RNAi Negative Control Duplexes with similar G/C content (Invitrogen) were used as a negative control.

RT-PCR

Total RNA was isolated from cultured EAhy926 using TRIzol (Invitrogen) according to the manufacturer's instructions. Complementary DNA was prepared using a reverse transcriptase–polymerase chain reaction (RT-PCR) kit (RETROscript; Ambion, TX, USA). PCR reactions were performed with *Taq* polymerase using the following specific primers. The primer sequences were as follows: NOXA1 sense primer: 5′-TGGGAGG TGCTACACAATGTG-3′, antisense primer: 5′-GACCTCTGT CTCTGCATCGA-3′; $p22^{phox}$ sense primer: 5′-GTTTGTGTG CCTGCTGGAGT-3′, antisense primer: 5′-TGGGCGGCTGCT TGATGGT-3′. NOXA1 cDNA amplification was performed in 35 cycles: sample were heated to 94°C for 1 min, cooled to 60°C for 1 min, and then heated at 72°C for 1 min. p22phox cDNA amplification was performed in 25 cycles: samples were heated to 94°C for 1 min, cooled to 59°C for 1 min, and then heated at 72°C for 1 min. PCR products were separated using 1% agarose gels stained with ethidium bromide and visualized under ultraviolet (UV) light. PCR products were purified and further analyzed by DNA sequencing using an ABI Prism BigDye Terminator Cycle Sequencing kit on an ABI Prism 310 Genetic Analyzer. To measure the production of each mRNA, RT-PCR for human glutaldehyde-3-phosphate dehydrogenase (GAPDH) was also performed (sense primer 5′-ACGGATTTGGTCGTATTGGGC-3′, antisense primer 5′-TTGACGGTGCCATGGAATTTG-3′).

Evaluation of Intracellular Reactive Oxygen Species by Dihydroethidium Methods

Intracellular ROS was detected with dihydroethidium (Molecular Probes, Eugene, OR, USA). A confluent monolayer cells were stimulated with angiotensin II (10^{-7} mol/L) (Sigma Chemical) or ox-LDL for 1 h. After stimulation, they were treated with dihydroethidium (2 μmol/L) for 20 min at 37°C in the dark. The fluorescence intensity was measured using a laser-scanning confocal imaging system, and quantified using ImageJ software (National Institutes of Health).

Statistical Analysis

Data are presented as mean ± *SE*. Statistical analysis was performed by analysis of variance followed by Fisher's probable least significant difference (PLSD) test. A p value of less than .05 was considered to be statistically significant.

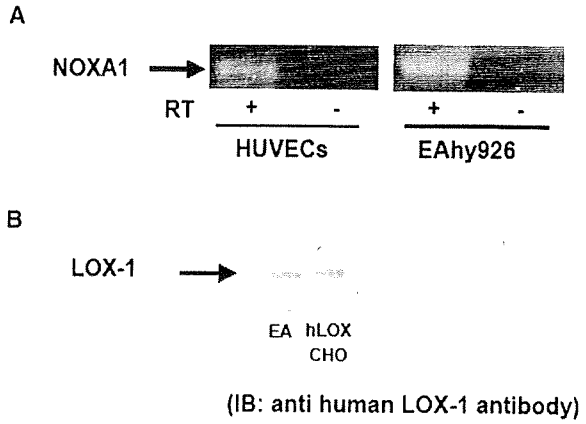

FIG. 1. Expression of NOXA1 and LOX-1 in human endothelial cells. RT-PCR confirmed the expression of NOXA1 in cultured HUVECs and its continuous cell line EAhy926 (*A*). Western blotting analysis confirmed the expression of LOX-1 in EAhy926. HLOX-CHO, which continuous expressed human LOX-1, was used as a positive control (*B*).

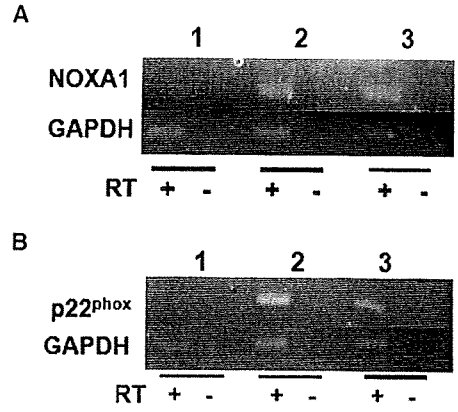

FIG. 2. Suppression of NOXA1 and $p22^{phox}$ by transfection of siRNA in endothelial cells. The expression of NOXA1 and $p22^{phox}$ were potently suppressed by their target siRNA. 1 = target Stealth RNAi; 2 = mock control, 3 = Stealth negative-control duplexes. Their mock control and scramble control had no effects (*A* and *B*).

RESULTS

NOXA1 and LOX-1 Were Expressed in Endothelial Cell Line

The expression of NOXA1, in human umbilical vein endothelial cells (HUVECs), was confirmed by RT-PCR. No RT-PCR product was present in the negative control in which RT was not performed. EAhy926, a continuous cell line of HUVECs, also expressed NOXA1 (Figure 1*A*). Sequencing of complementary DNA of NOXA1 obtained from HUVECs and EAhy926 were the same as reported before (data not shown) (Takeya et al. 2003). Thus, NOXA1 was expressed in endothelial cells. The expression of LOX-1 in EAhy926 was confirmed by Western blotting analysis. EAhy926 had the same sized band as hLOX-CHO cells, which permanently express human LOX-1 (Figure 1*B*).

NOXA1 and $p22^{phox}$ Were Essential for ROS Generation in Endothelial Cells

RT-PCR revealed that transfection with siRNA of NOXA1 and $p22^{phox}$ potently suppressed their expression in endothelial cells, whereas their mock control and scramble control had no effects (Figure 2).

Suppression of $p22^{phox}$ by siRNA significantly decreased the generation of intracellular ROS induced by ox-LDL (30 μg/mL) and angiotensin II (10^{-7}M) in endothelial cells evaluated by dihydroethidium method. Its mock control and scramble control had no effects (Figure 3). Similarly, the suppression of NOXA1 by siRNA induced a significant reduction of the generation of ROS (Figure 3).

The Expression of NOXA1 Was Increased by Ox-LDL in Endothelial Cells

The effect of ox-LDL on expression of NOXA1 was examined by RT-PCR. Incubation with ox-LDL for 12 h significantly increased the expression of NOXA1 in a dose-dependent manner (Figure 4*A*). Incubation with ox-LDL (30 μg/mL) moderately increased the expression of NOXA1 in a time-dependent manner, especially in 24 h (Figure 4*B*). Thus, ox-LDL not only increased the generation of intracellular ROS via LOX-1, but also enhanced the expression of NOXA1.

DISCUSSION

Vascular NAD(P)H oxidase, which regulates superoxide, plays an important role in pathogenesis of various cardiovascular disease (Kobayashi et al. 2003; Azumi et al. 2002; Brandes and Kreuzer 2005; Sorescu et al. 2002; Tojo et al. 2005). There is no direct evidence that NOXA1 is involved with endothelial NAD(P)H oxidase. The present investigation is the first study to demonstrate that NOXA1 is expressed in endothelial cells. Down-regulation of $p22^{phox}$ and NOXA1 by siRNA significantly suppressed the generation of intracellular ROS. Furthermore, the expression of NOXA1 was increased by ox-LDL in a time- and dose-dependent manner.

The active superoxide-generating subunit of NAD(P)H oxidase is the NOX protein. NOX1 activation requires membrane recruitment of NOXA1, which is normally mediated via binding to NOXO1. NOXO1 tethers to the $p22^{phox}$ even in the resting state. In the presence of NOXA1 and NOXO1, NOX1 produces superoxide without cell stimulants. The NOXA1-NOXO1 and NOXO1-$p22^{phox}$ interactions are both essential for NOX1 activity (Takeya et al. 2003; Miyano et al. 2006). On the other hand, NOXA1 as well as $p67^{phox}$ contains a small GTPase Rac-binding domain in the N-terminal region. The Rac-NOXA1 interaction at the membrane plays a crucial role in NOX1 activation. Rac directly participates in formation of the active NOX1 complex via binding to NOXA1 (Miyano et al. 2006; Ueyama et al. 2006). We previously demonstrated that the NAD(P)H oxidase is expressed in coronary arteries of patients with coronary artery disease, and $p22^{phox}$-based NAD(P)H oxidase plays a major

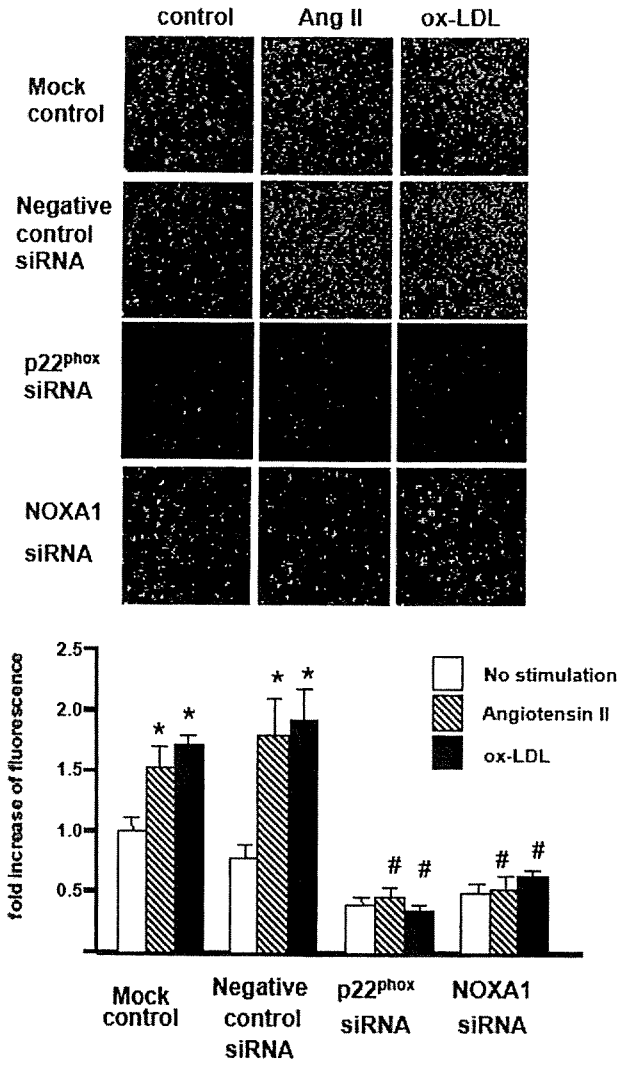

FIG. 3. The role of $p22^{phox}$ and NOXA1 to generate intracellular ROS in endothelial cells. Incubation with angiotensin II (10^{-7}M) or ox-LDL (30 μg/mL) induced the generation of intracellular ROS in endothelial cells, assessed by the dihydroethiduim methods. Suppression of $p22^{phox}$ by siRNA decreased the generation of intracellular ROS induced by angiotensin II or ox-LDL. Similarly, suppression of NOXA1 by siRNA induced a siginificant reduction of generation of ROS. Lower panels show quantitative analysis of the fluorescence intensity of dihydroethidium. $*p < .05$ versus no stimulation; $\#p < .05$ versus negative-control siRNA.

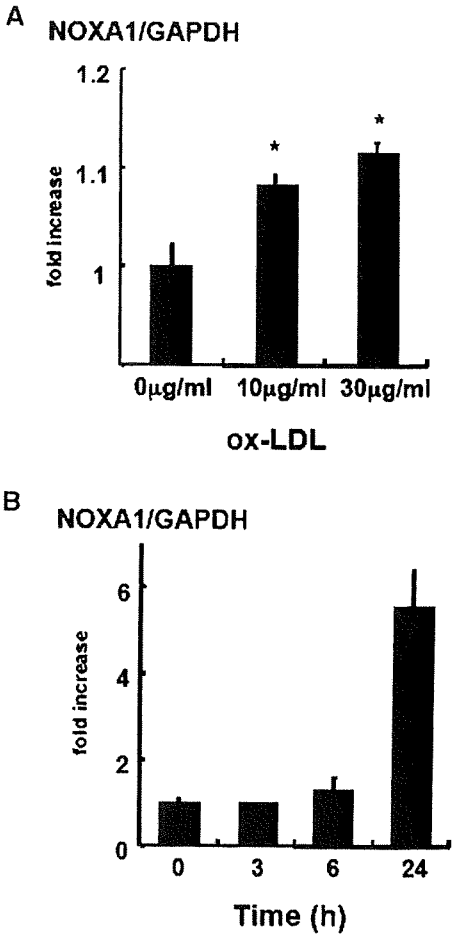

FIG. 4. The effects of ox-LDL on NOXA1 expression in endothelial cells. Endothelial cells were incubated with the indicated concentration of ox-LDL for 12 h (*A*) or incubated with ox-LDL (30 μg/mL) for the indicated time periods (*B*). After stimulation, expression of NOXA1 was assessed by RT-PCR. Data were plotted as mean ± *SE*. $*p < .01$ versus 0 μg/mL.

role in pathogenesis of atherosclerotic coronary artery disease (Kobayashi et al. 2003; Azumi et al. 2002). In the present investigation, NOXA1 was expressed in the endothelial cells and was essential on ROS generation. These findings suggest that not only endothelial $p22^{phox}$ but also endothelial NOXA1 is one of the quite important components of endothelial NAD(P)H oxidase, and that NOXA1 is a key player of in the pathogenesis of atherosclerotic coronary artery disease.

Interestingly, ox-LDL not only increased the generation of ROS via binding to LOX-1, but also enhances the expression of NOXA1 in a time- and dose-dependent manner in endothelial cells. Because NOXA1 is essential for the generation of ROS, it is interesting to speculate that there is a vicious cycle consisting of ox-LDL, NOXA-1, and LOX-1. That is to say, ox-LDL binds to LOX-1 and enhances the expression of NOXA1, then NOXA1 augments the generation of ROS. Furthermore, ROS induce the oxidative modification of LDL. In endothelial cells, the mechanism of generating ROS by LOX-1 is involved with endothelial NAD(P)H oxidase, especially NOX1, Rac, and NOXA1. NOXA1 is likely a key player, which links ox-LDL with the activation of endothelial NAD(P)H oxidase.

As described above, atherosclerotic cardiovascular disease is associated with oxidative stress. Clinical investigations show that coronary risk factors induced oxidative stress. Indeed, we demonstrated that the generation of ROS in coronary arteries of ischemic heart disease was markedly enhanced (Kobayashi et al. 2003; Azumi et al. 2002). Thus, oxidative stress may be a common pathway from coronary risk factors and atherosclerotic vascular diseases. Therefore, it can be thought that therapeutic interventions using antioxidant drugs can reduce the occurrence

of cardiovascular diseases (CVDs) and improve the survival and mortality of cardiovascular diseases. However, using antioxidants has not produced good results to prevent CADs in clinical trials, although there are few exceptions. Meta-analysis demonstrates that cardiovascular as well as cerebrovascular events did not differ between patients treated and those not treated with antioxidative vitamins (Hoogwerf and Young 2000; Lonn et al. 2001; Group HPSC 2002; Lee et al. 2005). Thus, at the present time, antioxidant drugs likely have no beneficial effect on cardiovascular disease. Precise reasons of the ineffectiveness of antioxidants for cardiovascular diseases remain to be elucidated. Besides harmful effects, ROS plays various physiological roles including host-defense system or intracellular signaling. Therefore, more specific agents may be necessary for the prevention and treatment for cardiovascular diseases. In the present investigation, the down-regulation of NOXA1 dramatically reduced the generation of ROS in endothelial cells. NOXA1 could be a novel therapeutic target of atherosclerosis-based heart disease from a view point of oxidative stress.

In conclusion, NOXA1 was expressed in vascular endothelial cells. Ox-LDL not only increased the generation of ROS via LOX-1, but also enhanced the expression of NOXA1. NOXA1 is likely a key player that links ox-LDL with the activation of endothelial NAD(P)H oxidase.

REFERENCES

Azumi H., Inoue N, Ohashi Y., Terashima M., Mori T., Fujita H., Awano K., Kobayashi K., Maeda K., Hata K., Shinke T., Kobayashi S., Hirata K., Kawashima S., Itabe H., Hayashi Y., Imajoh-Ohmi S., Itoh H., and Yokoyama M. (2002) Superoxide generation in directional coronary atherectomy specimens of patients with angina pectoris: Important role of NAD(P)H oxidase. *Arteriosclerosis, Thrombosis, and Vascular Biology*, **22**, 1838–1844.

Banfi B., Clark R.A., Steger K., and Krause K.H. (2003) Two novel proteins activate superoxide generation by the NADPH oxidase NOX1. *Journal of Biological Chemistry*, **278**, 3510–3513.

Brandes R.P., and Kreuzer J. (2005) Vascular NADPH oxidases: Molecular mechanisms of activation. *Cardiovascular Research*, **65**, 16–27.

Chen M., Kakutani M., Minami M., Kataoka H., Kume N., Narumiya S., Kita T., Masaki T., and Sawamura T. (2000) Increased expression of lectin-like oxidized low density lipoprotein receptor-1 in initial atherosclerotic lesions of Watanabe heritable hyperlipidemic rabbits. *Arteriosclerosis, Thrombosis, and Vascular Biology*, **20**, 1107–1115.

Cominacini L., Rigoni A., Pasini A.F., Garbin U., Davoli A., Campagnola M., Pastorino A.M., Lo Cascio V., and Sawamura T. (2001) The binding of oxidized low density lipoprotein (ox-LDL) to ox-LDL receptor-1 reduces the intracellular concentration of nitric oxide in endothelial cells through an increased production of superoxide. *Journal of Biological Chemistry*, **276**, 13750–13755.

Geiszt M., Lekstrom K., Witta J., and Leto T.L. (2003) Proteins homologous to p47phox and p67phox support superoxide production by NAD(P)H oxidase 1 in colon epithelial cells. *Journal of Biological Chemistry*, **278**, 20006–20012.

Geiszt M., and Leto T.L. (2004) The Nox family of NAD(P)H oxidases: Host defense and beyond. *Journal of Biological Chemistry*, **279**, 51715–51718.

Griendling K.K., Minieri C.A., Ollerenshaw J.D., Alexander R.W. (1994) Angiotensin II stimulates NADH and NADPH oxidase activity in cultured vascular smooth muscle cells. *Circulation Research*, **74**, 1141–1148.

Group H.P.S.C. (2002) MRC/BHF Heart Protection Study of antioxidant vitamin supplementation in 20,536 high-risk individuals: A randomised placebo-controlled trial. *Lancet*, **360**, 23–33.

Hoogwerf B.J., and Young J.B. (2000) The HOPE study. Ramipril lowered cardiovascular risk, but vitamin E did not. *Cleveland Clinic Journal of Medicine*, **67**, 287–293.

Kataoka H., Kume N., Miyamoto S., Minami M., Moriwaki H., Murase T., Sawamura T., Masaki T., Hashimoto N., and Kita T. (1999) Expression of lectinlike oxidized low-density lipoprotein receptor-1 in human atherosclerotic lesions. *Circulation*, **99**, 3110–3117.

Kobayashi S., Inoue N., Ohashi Y., Terashima M., Matsui K., Mori T., Fujita H., Awano K., Kobayashi K., Azumi H., Ejiri J., Hirata K., Kawashima S., Hayashi Y., Yokozaki H., Itoh H., and Yokoyama M. (2003) Interaction of oxidative stress and inflammatory response in coronary plaque instability: Important role of C-reactive protein. *Arteriosclerosis, Thrombosis, and Vascular Biology*, **23**, 1398–1404.

Lambeth J.D. (2004) NOX enzymes and the biology of reactive oxygen. *Nature Reviews Immunology*, **4**, 181–189.

Lee I.M., Cook N.R., Gaziano J.M., Gordon D., Ridker P.M., Manson J.E., Hennekens C.H., and Buring J.E. (2005) Vitamin E in the primary prevention of cardiovascular disease and cancer: The Women's Health Study: A randomized controlled trial. *Journal of the American Medical Association*, **294**, 56–65.

Li L., Roumeliotis N., Sawamura T., and Renier G. (2004) C-reactive protein enhances LOX-1 expression in human aortic endothelial cells: Relevance of LOX-1 to C-reactive protein-induced endothelial dysfunction. *Circulation Research*, **95**, 877–883.

Lonn E., Yusuf S., Dzavik V., Doris C., Yi Q., Smith S., Moore-Cox A., Bosch J., Riley W., and Teo K. (2001) Effects of ramipril and vitamin E on atherosclerosis: The study to evaluate carotid ultrasound changes in patients treated with ramipril and vitamin E (SECURE). *Circulation*, **103**, 919–925.

Miyano K., Ueno N., Takeya R., and Sumimoto H. (2006) Direct involvement of the small GTPase Rac in activation of the superoxide-producing NADPH oxidase Nox1. *Journal of Biological Chemistry*, **281**, 21857–21868.

Nagase M., Kaname S., Nagase T., Wang G., Ando K., Sawamura T., and Fujita T. (2000) Expression of LOX-1, an oxidized low-density lipoprotein receptor, in experimental hypertensive glomerulosclerosis. *Journal of the American Society of Nephrology*, **11**, 1826–1836.

Sawamura T., Kume N., Aoyama T., Moriwaki H., Hoshikawa H., Aiba Y., Tanaka T., Miwa S., Katsura Y., Kita T., and Masaki T. (1997) An endothelial receptor for oxidized low-density lipoprotein. *Nature*, **386**, 73–77.

Sorescu D., Weiss D., Lassegue B., Clempus R.E., Szocs K., Sorescu G.P., Valppu L., Quinn M.T., Lambeth J.D., Vega J.D., Taylor W.R., and Griendling K.K. (2002) Superoxide production and expression of nox family proteins in human atherosclerosis. *Circulation*, **105**, 1429–1435.

Takeya R., and Sumimoto H. (2003) Molecular mechanism for activation of superoxide-producing NADPH oxidases. *Molecules and Cells*, **16**, 271–277.

Takeya R., Ueno N., Kami K., Taura M., Kohjima M., Izaki T., Nunoi H., and Sumimoto H. (2003) Novel human homologues of p47phox and p67phox participate in activation of superoxide-producing NADPH oxidases. *Journal of Biological Chemistry*, **278**, 25234–25246.

Tojo T., Ushio-Fukai M., Yamaoka-Tojo M., Ikeda S., Patrushev N., and Alexander R.W. (2005) Role of gp91phox (Nox2)-containing NAD(P)H oxidase in angiogenesis in response to hindlimb ischemia. *Circulation*, **111**, 2347–2355.

Ueyama T., Geiszt M., and Leto T.L. (2006) Involvement of Rac1 in activation of multicomponent Nox1- and Nox3-based NADPH oxidases. *Molecular and Cellular Biology*, **26**, 2160–2174.

Novel Gene Silencer Pyrrole-Imidazole Polyamide Targeting Lectin-Like Oxidized Low-Density Lipoprotein Receptor-1 Attenuates Restenosis of the Artery After Injury

En-Hui Yao, Noboru Fukuda, Takahiro Ueno, Hiroyuki Matsuda, Koichi Matsumoto, Hiroki Nagase, Yoshiaki Matsumoto, Ayako Takasaka, Kazuo Serie, Hiroshi Sugiyama, Tatsuya Sawamura

Abstract—Lectin-like oxidized low-density lipoprotein receptor-1 (LOX-1) is a membrane protein that can support the binding, internalization, and proteolytic degradation of oxidized low-density lipoprotein. The LOX-1 expression increases in the neointima after balloon injury. To develop an efficient compound to inhibit LOX-1, we designed and synthesized a novel gene silencer pyrrole-imidazole (PI) polyamide targeting the rat LOX-1 gene promoter (PI polyamide to LOX-1) to the activator protein-1 binding site. We examined the effects of PI polyamide to LOX-1 on the LOX-1 promoter activity, the expression of LOX-1 mRNA and protein, and neointimal hyperplasia of the rat carotid artery after balloon injury. PI polyamide to LOX-1 significantly inhibited the rat LOX-1 promoter activity and decreased the expression of LOX-1 mRNA and protein. After balloon injury of the arteries, PI polyamide to LOX-1 was incubated for 10 minutes. Fluorescein isothiocyanate–labeled PI polyamide was distributed to almost all of the nuclei in the injured artery. PI polyamide to LOX-1 (100 μg) significantly inhibited the neointimal thickening by 58%. PI polyamide preserved the re-endothelialization in the injured artery. PI polyamide significantly inhibited the expression of LOX-1, monocyte chemoattractant protein-1, intercellular adhesion molecule-1, and matrix metalloproteinase-9 mRNAs in the injured artery. The synthetic PI polyamide to LOX-1 decreased the expression of LOX-1 and inhibited neointimal hyperplasia after arterial injury. This novel gene silencer PI polyamide to LOX-1 is, therefore, considered to be a feasible agent for the treatment of in-stent restenosis. (***Hypertension***. **2008;52:86-92.)**

Key Words: basic science ■ endothelium ■ gene therapy ■ cytokines ■ polyamide ■ LOX-1 ■ restenosis

Coronary artery restenosis after angioplasty occurs in ≈30% of all patients.[1,2] Despite the widespread use of intracoronary stents, in-stent restenosis remains a major clinical problem, occurring in ≤50% of high-risk patients.[3] The development of neointimal hyperplasia after arterial injury contributes to the pathogenesis of restenosis. Several factors are involved in the initiation and progression of neointimal hyperplasia. Coronary arterial diseases are known to be associated with several risks, such as dyslipidemia, hypertension, smoking, and diabetes. A pivotal common factor in these risks is oxidative stress, which also induces restenosis of the coronary artery.[4]

The oxidized low-density lipoprotein (ox-LDL) is recognized to be a major cause of endothelial dysfunction in atherogenesis.[5] Lectin-like ox-LDL receptor-1 (LOX-1), a receptor for ox-LDL, is a membrane protein that is expressed in both the vascular endothelium and vascular-rich organs. LOX-1 can support the binding, internalization, and proteolytic degradation of ox-LDL.[6] The LOX-1 expression has been reported to significantly increase in the neointima after balloon injury in various animal models of neointimal hyperplasia, such as rats and rabbits. Hinagata et al[7] reported neointimal hyperplasia after balloon injury to be markedly attenuated by treatment with anti–LOX-1 antibody in a rat model. These findings suggest that LOX-1 expressed in the neointima is involved in the pathogenesis of restenosis after arterial injury, and, therefore, LOX-1 may be a potential therapeutic target for the prevention/treatment of neointimal hyperplasia and restenosis after arterial injury.

Pyrrole-imidazole (PI) polyamide is a powerful gene-regulating compound that can inhibit protein, including enhancers or repressors, DNA binding, and interaction by binding to the minor groove of double-helical DNA with high affinity and specificity.[8] PI polyamide was first identified from duocarmycin A and distamycin A, which recognize and bind DNA with sequence specificities and are small synthetic molecules com-

Received February 29, 2008; first decision March 26, 2008; revision accepted May 2, 2008.

From the Division of Nephrology Hypertension and Endocrinology, Department of Medicine (E.-H.Y., N.F., T.U., H.M., K.M.), Division of Cancer Genetics, Department of Advanced Medical Science (H.N.), and Department of Cardiovascular Surgery (A.T.), Nihon University School of Medicine, Tokyo; Advanced Research Institute of the Sciences and Humanities (N.F., H.M., H.N.), Nihon University, Tokyo; Department of Clinical Pharmacokinetics (Y.M.), College of Pharmacy, Nihon University, Chiba; College of Engineering (K.S.), Nihon University Graduate School, Koriyama, Fukushima; Department of Chemistry (H.S.), Graduate School of Science, Kyoto University, Kyoto; and the Department of Vascular Physiology (T.S.), National Cardiovascular Center Research Institute, Osaka, Japan.

Correspondence to Noboru Fukuda, Division of Nephrology Hypertension and Endocrinology, Department of Medicine, Nihon University School of Medicine, Ooyaguchi-kami 30-1, Itabashi-ku, Tokyo 173-8610, Japan. E-mail fukudan@med.nihon-u.ac.jp

Hypertension **is available at http://hyper.ahajournals.org** **DOI: 10.1161/HYPERTENSIONAHA.108.112797**

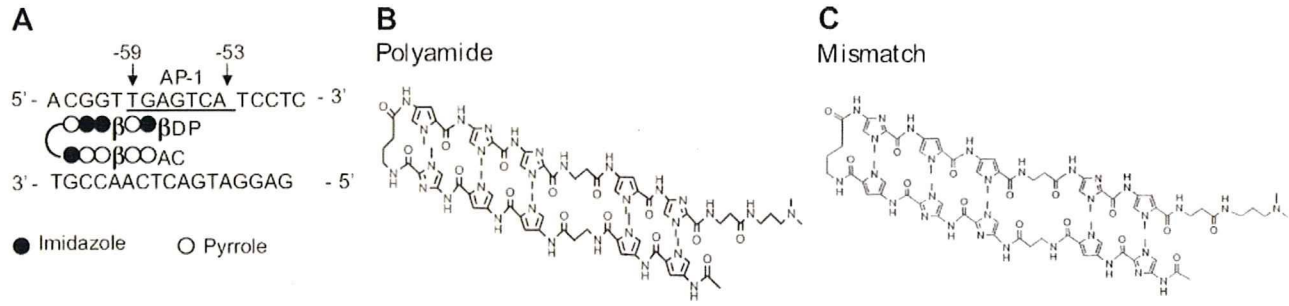

Figure 1. A, The target site of synthesized PI polyamide targeting rat LOX-1 promoter (PI polyamide to LOX-1). PI polyamide to LOX-1 was designed to span the boundary of the AP-1 binding site (−63 to −58) of the LOX-1 promoter. B and C, The structure of synthesized PI polyamide targeting rat LOX-1 promoter and mismatch polyamide. The mismatch polyamide was composed of scramble polyamides. Molecular weight=1669.

posed of the aromatic rings of *N*-methylpyrrole and *N*-methylimidazole amino acids.[9,10] PI polyamides are resistant to nucleases and do not require any particular delivery systems.[11] Various types of sequence-specific DNA-binding PI polyamides have been developed to control gene expression.[12] DNA recognition depends on a code of side-by-side pairing of pyrrole and imidazole in the minor groove. A pairing of imidazole opposite pyrrole targets the G-C bp, and pyrrole-imidazole targets the C-G bp. Pyrrole-pyrrole degenerately targets the T-A bp and A-T bp.[10] We have reported previously that PI polyamide targeted to the transforming growth factor-β1 promoter for progressive renal diseases significantly inhibited the transforming growth factor-β1 promoter activity and the expressions of transforming growth factor-β1 mRNA and protein in mesangial cells.[13] These findings suggest that the synthetic PI polyamides targeting gene promoter may, therefore, be feasible agents for the treatment of such diseases.

In this study, to develop a new agent for the treatment of restenosis after angioplasty, we designed a PI polyamide targeting rat LOX-1 gene promoter (PI polyamide to LOX-1) and examined its effects on LOX-1 expression and neointimal formation after balloon arterial injury in a rat model.

Methods

Synthesis of Polyamide Targeting Rat LOX-1

PI polyamide to LOX-1 was designed to span the boundary of the activator protein-1 (AP-1) binding site (−63 to −58) of the LOX-1 promoter (Figure 1A and 1B). A mismatch polyamide was used as a negative control; it was designed not to bind transcription binding sites of the promoter (Figure 1C). PI polyamides were synthesized by Gentier Biosystems Inc, according to methods described previously.[14]

Cell Culture

Rat aortic endothelial cells (Cell Applications) were inoculated on the coated plate and cultured in rat endothelial cell growth medium containing heparin, hydrocortisone, human epidermal growth factor, human fibroblast growth factor, dibutyryl cAMP, and FBS (5% vol/vol final concentration) in a CO_2 incubator. After reaching 90% confluence, the endothelial cells were incubated in serum-free medium for 24 hours, and then the medium was exchanged for a new medium at the start of the experiments.

Reverse Transcription and PCR Analysis

The total RNA was isolated and reverse transcribed as described previously.[15] The primers used to amplify monocyte chemoattractant protein-1 (MCP-1), matrix metallopeptidase-9 (MMP-9), and adhesion molecule-1 (ICAM-1) are listed in Table S1 (available online at http://hyper.ahajournals.org.). 18S ribosomal RNA was amplified as an internal control. PCR was performed according to the profiles shown in Table S2. PCR was performed in a DNA thermal cycler (GeneAmp PCR System 2700, Applied Biosystems). The quality and concentration of the amplified PCR products were determined using an Agilent 2100 Bioanalyzer (Agilent).

Arterial Injury and Treatment With Polyamide

This study confirmed to the standards of the Guide for the Care and Use of Laboratory Animals published by the National Institutes of Health. Male Wistar rats (Charles River Breeding Laboratories) weighing 300 to 350 g were used in all of the experiments. The rats were anesthetized by an IP injection of pentobarbital (100 mg/kg of body weight). The left carotid artery was isolated, and a Fogarty 2F embolectomy catheter (Baxter Healthcare) was introduced through the external carotid arteriotomy incision, advanced to the aortic arch, inflated to produce moderate resistance, and then gradually withdrawn 3 times to produce a distending and de-endothelializing injury.[16] The catheter was removed and the external carotid branch ligated. For local delivery, PI polyamide to LOX-1 or mismatch polyamide was diluted to 10 or 100 μg in 50 μL of saline, and they were injected and maintained in the artery for 10 minutes. After the incubation period, the solution was evacuated, the artery was washed with PBS 3 times, and then the blood flow through the common carotid artery was re-established.

Distribution of Fluorescein-Labeled Polyamide in Injured Artery

To assess the distribution of the polyamide in the carotid artery after the balloon injury, 100 μg of fluorescein isothiocyanate (FITC)–labeled PI polyamide to LOX-1 was incubated within the lumen of the artery for 10 minutes. The vessels were harvested 30 minutes, 2 hours and 24 hours later. Frozen specimens were made and then examined by fluorescence microscopy.

Morphometric Analysis of Neointimal Hyperplasia

The effect of polyamide on neointimal formation was measured as described previously.[17] The rats were euthanized by a lethal injection of sodium pentobarbital (IP, 100 mg/kg of body weight) at 21 days after balloon injury and then perfused with saline followed by 10% formalin at physiological pressure. For immunohistochemistry and a morphometric analysis, the arteries were fixed in 100% methanol overnight, and the middle one third of the common carotid artery was then cut into 4 segments and embedded in paraffin. The specimens were cross-sectioned at a thickness of 3 μm and stained with hematoxylin-eosin. The intima/media cross-sectional area ratios were determined using a computerized apparatus and the National Institutes of Health Image software program (version 1.57).

Immunohistochemistry

Paraffin blocks of the segments of the carotid arteries were used for the immunohistochemistry assay. LOX-1 expression was identified

with goat polyclonal anti–LOX-1 antibody (1:200, Santa Cruz), and incubated with fluorescein-conjugated chicken antigoat antibody (1:500, Invitrogen). After washing with PBS, the sections were incubated with Hoechst 33342 and then viewed by a laser scanning confocal imaging system.

Statistical Analyses

The values are reported as the means±SEMs. Student *t* test was used for unpaired data. Two-way ANOVA was also used. $P<0.05$ was considered to be statistically significant.

Results

Rat LOX-1 Promoter Activity

To identify DNA elements for regulation of rat LOX-1 promoter activation, 4 deletion constructs of the rat LOX-1 promoter were generated (Figure S1A). These constructs were transiently transfected into HEK-293 cells treated without or with phorbol 12-myristate 13-acetate (PMA) and measured for luciferase activity. PMA-induced activity was observed in −2385Luc, −1978Luc, −1323Luc, and −128Luc. The luciferase activity of these constructs significantly ($P<0.05$) increased with PMA by 2.8- to 3.2-fold in comparison with the basal activity, whereas the promoterless construct pGL3-basic was unresponsive. These results indicate that the sequence from −128 to +24 is important for PMA-induced activation of the LOX-1 promoter. We searched for transcription factor–binding sites with TFSEARCH and found an AP-1 site (5′-TGAGTCA-3′) lying between bp −59 and −53. To further confirm this AP-1 site on the LOX-1 promoter necessary for LOX-1 promoter activity in response to PMA, a 2-bp mutated construct was made in the luciferase reporter plasmid −128Luc. The luciferase activity in the HEK-293 cells transfected with these mutants revealed that mutation of the AP-1 site abolished the effect of PMA on LOX-1 promoter activity (Figure S1B). Therefore, this AP-1 site was essential for promoter activation. The PI polyamide to LOX-1 was then designed to interfere with this site.

Binding of Polyamide to Target DNA

The binding affinity and specificity of polyamide to target DNA were determined by gel shift assay (Figure S2). PI polyamide to LOX-1 bound the target double-stranded DNA. However, PI polyamide to LOX-1 did not bind to the 2-bp mutated double-stranded DNA. The mismatch polyamide did not bind to the double-stranded DNA.

Effect of PI Polyamide to LOX-1 on LOX-1 Promoter Activity

PMA (0.1 μmol/L) markedly increased the luciferase activity in HEK-293 cells transfected with LOX-1 promoter plasmid.

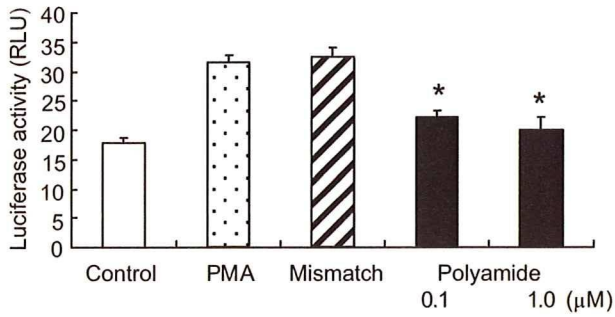

Figure 2. The effect of PI polyamide targeting rat LOX-1 promoter (PI polyamide to LOX-1) on the LOX-1 promoter activity. HEK-293 cells were transfected with recombinant LOX-1 promoter plasmids; 24 hours after transfection, cells were incubated with either PI polyamide or mismatch polyamide in the presence or absence of 0.1 μmol/L of PMA; thereafter, the luciferase activity in the cell extracts was determined. The data are the means±SEMs (n=8). *$P<0.05$ vs treatment with PMA.

Treatment consisting of 0.1 and 1.0 μmol/L of PI polyamide to LOX-1 significantly ($P<0.05$) inhibited the LOX-1 promoter activity. However, the mismatch polyamide (1 μmol/L) did not affect the LOX-1 promoter activity (Figure 2).

Effect of PI Polyamide to LOX-1 on the Expressions of LOX-1 mRNA and Protein in Cultured Rat Endothelial Cells

The expression of LOX-1 mRNA and protein was significantly ($P<0.05$) increased with PMA. PI polyamide to LOX-1 significantly ($P<0.05$) decreased the amount of LOX-1 mRNA and protein. However, the mismatch polyamide did not affect the amount of LOX-1 mRNA and protein (Figure S3A and S3B).

Distribution of PI Polyamide to LOX-1 in Injured Artery

Figure 3 shows the distribution of FITC-labeled PI polyamide to LOX-1 in rat carotid artery after balloon injury. The FITC-labeled PI polyamide was not seen and then was uptaken into the entire wall of the injured artery at 30 minutes after injury. Thereafter, the FITC-labeled PI polyamide remained and strongly localized in the nuclei of midlayer smooth muscle by 24 hours.

Effect of PI Polyamide to LOX-1 on Neointimal Thickening

Figure 4 shows the effect of PI polyamide to LOX-1 on neointimal thickening in rat carotid artery at 21 days after balloon injury. Both 10 and 100 μg of PI polyamide to

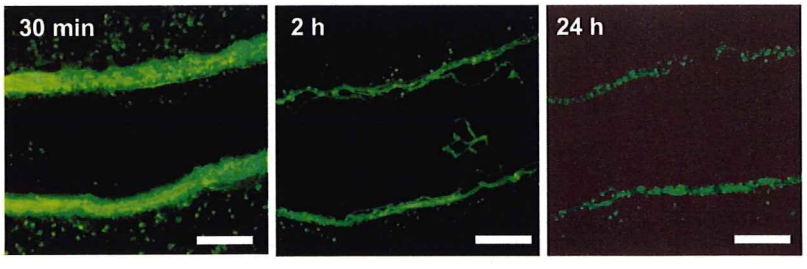

Figure 3. Distribution of FITC-labeled PI polyamide targeting rat LOX-1 promoter (PI polyamide to LOX-1) in injured carotid artery. FITC-labeled polyamide (100 μg) was incubated within the lumen of artery for 10 minutes. The vessels were harvested 30 minutes, 2 hours, or 24 hours later and frozen specimens were made and were examined by fluorescence microscopy. Scale bar represents 1 mm.